ADVANCED FUNCTIONAL MATERIALS
www.afm-journal.de

Translational Neuroelectronics

Patricia Jastrzebska-Perfect, Shilpika Chowdhury, George D. Spyropoulos, Zifang Zhao, Claudia Cea, Jennifer N. Gelinas, and Dion Khodagholy**

Neuroelectronic devices are critical for the diagnosis and treatment of neuropsychiatric conditions, and are hypothesized to have many more applications. A wide variety of materials and approaches have been utilized to create innovative neuroelectronic device components, from the tissue interface and acquisition electronics to interconnects and encapsulation. Although traditional materials have a strong track record of stability and safety within a narrow range of use, many of their properties are suboptimal for chronic implantation in body tissue. Material advances harnessed to form all the components required for fully integrated neuroelectronic devices hold promise for improving the long-term efficacy and biocompatibility of these devices within physiological environments. Here, it is aimed to provide a comprehensive overview of materials and devices used in translational neuroelectronics, from acquisition and stimulation interfaces to methods for power delivery and real time processing of neural signals.

1. Clinical Applications of Neuroelectronics

To appropriately diagnose and treat disorders of the nervous system, it is critical to be able to accurately sense signals from the body that indicate the nature of the dysfunction and subsequently interact with the body to ameliorate the dysfunction and restore a physiologic state. Components of the nervous system communicate using electrical and chemical signals, which can be manipulated to achieve therapeutic effects. Therefore, the potential for use of bioelectronic devices to acquire, process, and alter neurophysiological signals is high. We will first briefly provide an overview of the electrical and chemical signals that contribute to diagnosis of neurologic disease and the current modalities available for treatment (**Figure 1**A–F). Advancements to all facets of these processes can improve clinical care of patients with neuropsychiatric diseases.

1.1. Diagnostics and Biomarkers

Understanding neurological disorders can be achieved using a range of biological indicators in different neurological systems. Though noninvasive diagnostics are possible, high resolution information is often collected using invasive electrical and chemical measurements.

1.1.1. Brain

Although individual neurons in the brain communicate via action potentials, these signals can only be detected and their origin tagged to a specific neuron by miniaturized recording electrodes that are located within hundreds of micrometers from the cell.[1] The material and procedural requirements of acquiring such data on a scale that is relevant to brain function have thus far precluded its use in clinical diagnostics. Due to the organization of brain neurons into layers and nuclei, higher amplitude electrical signals are generated by incoming synaptic activity to a large population of neurons. Such signals undergo spatial summation and can be detected at much greater distances from the neurons as oscillatory patterns and waveforms ranging between 0.5 and 500 Hz.[2] Many characteristics of brain function can be gleaned from acquiring these electrical potentials, with the spatial and temporal resolution of the data dependent on whether it is recorded from the surface of the scalp, surface of the brain, or within brain tissue.

Noninvasive: Noninvasive methods of recording brain activity are frequently used in clinical neurology, and include electroencephalography (EEG) and magnetoencephalography (MEG).

In the case of EEG, 19 electrodes are placed at standardized positions on the surface of the scalp to detect fluctuations in voltage in the range of 10–100 μV. Oscillatory activity with a frequency of greater than 40 Hz is typically difficult to resolve with EEG due to its restricted spatial distribution and low signal amplitude. With advanced signal processing techniques, it is sometimes possible to detect high frequency patterns,[3] but these approaches are not yet commonly employed in clinical

P. Jastrzebska-Perfect, S. Chowdhury, Dr. G. D. Spyropoulos, Dr. Z. Zhao, C. Cea, Dr. D. Khodagholy
Department of Electrical Engineering
Columbia University
New York, NY 10027, USA
E-mail: dk2955@columbia.edu
Dr. J. N. Gelinas
Department of Neurology
Columbia University Medical Center
New York, NY 10032, USA
E-mail: jng2146@cumc.columbia.edu
Dr. J. N. Gelinas
Institute for Genomic Medicine
Columbia University Irving Medical Center
New York, NY 10032, USA
The ORCID identification number(s) for the author(s) of this article can be found under https://doi.org/10.1002/adfm.201909165.

DOI: 10.1002/adfm.201909165

practice. In addition, electrical potentials that involve a small area of neural tissue, or are located deep within the brain, do not appear on EEG. It has been estimated that up to 6 cm^2 of neural tissue must be relatively synchronously active to generate patterns that are visible on EEG.[4] Because many different configurations of electrical potential patterns within the brain could generate a similar appearance on the surface, EEG also suffers from the "inverse problem" (whereby multiple combinations of a set of parameters may result in the same outcome), leading to the potential for inaccurate localization of EEG signals to brain structures.[5] Despite these limitations, EEG is a powerful tool for acquiring real-time information about brain function. The most common EEG diagnostic applications are in epilepsy, altered states of consciousness, and brain lesions. EEG is the first-line investigation when a diagnosis of epilepsy is considered, because the hypersynchronous neural firing patterns characteristic of this disease are often apparent.[6] Capturing epileptic activity on EEG facilitates classification of a patient's epilepsy and can guide the most appropriate treatment. However, EEG offers insufficient spatiotemporal resolution for localization of epileptic brain regions in a subset of patients who may require invasive monitoring (see below) to enable the most appropriate treatment. In patients with altered mental status, EEG can suggest brain structures most affected, provide clues as to the cause of the patient's symptoms, and in some cases provide prognostic information about how likely the patient is to recover from a neurologic insult.[7] Focal brain lesions result in slowing of oscillation frequencies on EEG, but the role of this diagnostic modality has decreased with the widespread availability of computerized neuroimaging. For all of these clinical scenarios, patients often require prolonged EEG monitoring (days to weeks) to capture appropriate diagnostic information, monitor response to treatment, and/or allow for early detection of neurologic complications in critical illness.[8] Therefore, the ability to stably record high quality EEG without causing side effects, such as skin breakdown at sites of electrode placement, is highly clinically desirable.

MEG acquires the magnetic rather than electric signals generated by population activity of neurons in the brain. Because the magnetic field is orthogonal to the electric field, MEG is better able to detect signals arising from fields that are tangential to the scalp. It is also less attenuated by the structures, cerebrospinal fluid, dura, skull, subcutaneous tissue, located between neurons and recording electrodes. Clinically, MEG has been mainly used to supplement and refine the localization of epileptic foci within the brain.[9]

Invasive: Some patients with focal epilepsy that is refractory to treatment with medicatins have the potential to benefit from surgical resection of the brain tissue responsible for generating seizures. When the combination of seizure manifestations, noninvasive electrophysiologic studies, and neuroimaging are insufficient to clearly define where this tissue is located or its boundaries, invasive monitoring of brain signals is considered.[10] Intracranial EEG (iEEG) involves placing electrodes on the cortical surface, in the form of grid arrays or strips, and/or inserting electrodes in the form of a rigid shank with multiple contacts directly into brain tissue. These electrodes may be placed acutely for a short time during a neurosurgical procedure to guide tissue resection and allow intraoperative monitoring, or semichronically for a period of up to two weeks during which time the patient remains in the hospital. iEEG has the benefit of enhanced spatiotemporal resolution, and permits more precise localization of epileptic activity than noninvasive methods[11] and may help to characterize dysfunction of the interictal neural network.[12] Current clinical iEEG technology does not permit acquisition of action potentials despite the proximity to brain tissue, but high frequency oscillations (several hundred Hz) can be reliably detected and used to aid localization of epileptic foci.[13] Evidence suggests that the ability to detect action potentials could improve this localization further, but no clinical trials of devices with this capacity have been performed, so the practical benefit to patients is unknown.[14] iEEG does carry more risk, with 1–4% of patients experiencing a complication related to the procedure such as bleeding, brain swelling, and infection.[15] As

Jennifer N. Gelinas obtained her M.D./Ph.D. at the University of Alberta. She completed residency in pediatric neurology at the University of British Columbia and an epilepsy fellowship at NYU Langone Medical Center (NYULMC). Her postdoctoral research fellowship at NYULMC investigated physiologic and epileptic neural networks using in vivo electrophysiology. She is an assistant professor in the Department of Neurology and Institute for Genomic Medicine at Columbia University Irving Medical Center. Her research focuses on the neurobiology of cognitive functions, especially as related to neuropsychiatric disease.

Dion Khodagholy is an assistant professor in the Department of Electrical Engineering at Columbia University in New York City. He received his Master's degree from the University of Birmingham (UK) in electronics and telecommunication engineering. This was followed by a second Master's degree in microelectronics at the Ecole des Mines. He attained his Ph.D. in microelectronics at the Department of Bioelectronics (BEL) of the Ecole des Mines (France). His postdoctoral research at New York University, Langone Medical Center was focused on large-scale cortical acquisition and analysis. His research explores the interface of electronics and the brain in the context of both applied and discovery sciences.

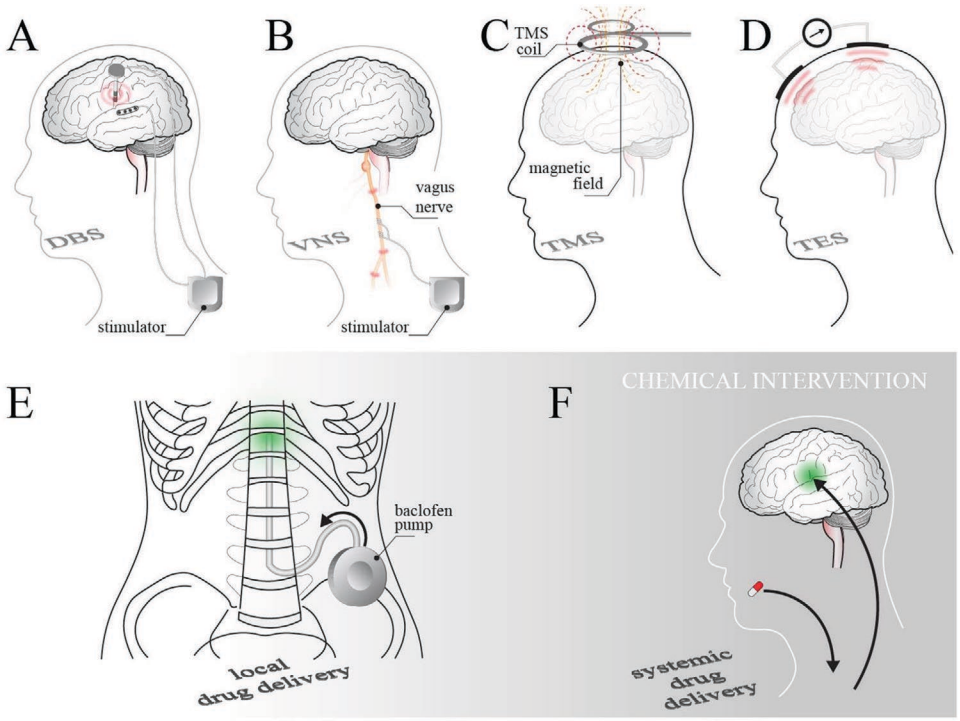

Figure 1. Common neurological clinical intervention approaches. A) Deep-brain stimulation (DBS) involves an implantable electrode connected to a remotely placed stimulator through leads routed subcutaneously. B) Vagal nerve stimulation (VNS) involves an electrode cuff wrapped around the vagus nerve and connected to an implanted stimulator. C) Transcranial magnetic stimulation (TMS) involves placement of magnetic coils above a brain region to be stimulated. D) Transcranial electrical stimulation (TES) involves placement of electrodes on the scalp over a brain region to be stimulated. E) Implantable pumps allow for localized, controlled drug delivery to the nervous system. F) Systemic drug delivery requires pharmacologic agents to undergo first pass metabolism and cross the blood–brain barrier before being able to modulate the central nervous system.

such, advancements that improve the spatiotemporal resolution of iEEG and decrease the associated morbidity are critical for improving care of patients who require this procedure.

1.1.2. Muscle

Muscle function is assessed by needle electromyography (EMG), a procedure that involves insertion of a concentric or monopolar needle through the skin and into a muscle to record muscle fiber action potentials. The amplitude, waveform duration and number of phases, firing rate and pattern, and stability of the action potentials identify when neurologic diseases involve motor neurons, motor nerves, or muscle. These properties typically identify the disease type, narrowing further investigations to establish a specific diagnosis.[16] In the case of a neuromuscular disorder, repeated studies over time can track disease progression or recovery.[17] Because sufficient spatiotemporal resolution can only be acquired by using penetrating electrodes, EMG is difficult to perform in patients who cannot tolerate the discomfort associated with it, such as children.

1.1.3. Nerve

Nerve function can be assayed by applying electrical stimulation through electrodes placed on the skin to elicit action potentials (nerve conduction studies, NCS). The combined action potential response is recorded using electrodes placed on the skin over muscle (motor nerves) or the course of a cutaneous nerve (sensory nerves). Analyzing the amplitude of the response provides insight into the number of axons that are conducting between the stimulating and recording points. The latency of the response after stimulation provides an estimate of the conduction velocity of the nerve, and the duration of the waveform adds information regarding how action potentials are being conducted along the nerve.[18] NCS provide important diagnostic information when patients experience motor and sensory symptoms, identifying loss of nerve fibers or impaired ability to conduct action potentials. When a disease process affecting the nerves is diagnosed, such as a demyelinating condition or toxic exposure, NCS can also be used to track recovery over time.[19]

1.1.4. Spinal Fluid Examination

Direct examination of the cerebrospinal fluid (CSF), which protects and chemically communicates with brain and spinal cord tissue, has been critical for diagnosis and management of neurologic disease for over a century. It is most useful in identifying intracranial infection, bleeding, cancer, metabolic disorders, and changes in intracranial pressure. Because obtaining CSF requires performing an invasive procedure,

lumbar puncture, the amount of fluid available for analysis and the capacity for serial sampling using current techniques is limited. Quantification of red and white blood cells, protein, and glucose within the CSF is typically performed, along with culture or immunologic studies looking for the presence of microorganisms. Studies aimed at identifying disorders of neurometabolism or autoimmunity can also be performed. Importantly, changes in these values over time are often critical to assay response to treatment, such as in patients receiving antivirals to treat encephalitis or those undergoing chemotherapy for brain cancer.[20] Bioelectronic devices capable of serially sampling small amounts of CSF and providing trends in quantification of key assays would prevent the requirement of performing multiple invasive procedures in these often critically ill patients.

1.2. Intervention and Treatment

1.2.1. Chemical Treatment

The majority of neurologic diseases are currently treated with medications. However, several challenges are encountered when trying to produce a desired pharmacologic response in the central nervous system. First, drug concentration within the brain is dependent upon the method of administration. Orally administered drugs can be extensively metabolized in the liver (first-pass metabolism) before reaching the brain, resulting in up to 75% of the administered dose never accessing systemic circulation.[20] Some drugs can be designed for sublingual, intranasal, or transdermal administration to avoid first-pass metabolism, but in order to reach brain tissue they still must cross the blood–brain barrier. The endothelial cells that make up the blood–brain barrier are tightly sealed to one another, preventing diffusion of most substances from blood into the brain. Drugs that are lipophilic, nonpolar, and have small molecular weight are most likely to cross the blood–brain barrier. Even if this barrier is crossed, the brain possesses carrier-mediated efflux systems that transport a wide variety of substances out of the brain, limiting drug accumulation.[21,22] To bypass the blood–brain barrier, drugs can be injected intrathecally (directly into the cerebrospinal fluid). This approach requires a lumbar puncture to be performed, and the associated pain and procedural risks limit its use to life-threatening conditions, such as pediatric leukemia, that involve the central nervous system.

Implantable drug delivery systems can circumvent some of these challenges, and offer opportunities for application of bioelectronic devices. Programmable pumps, such as the SynchroMed Intrathecal Pump by Medtronic PLC, are used to chronically deliver medications for pain and spasticity management.[23] The pump is implanted subcutaneously in the abdomen, with a small tube placed in the intrathecal space. The drug is continuously administered at a low rate, but some pumps can now be programmed by external magnetic signals to allow adjustment of flow. These pumps store 20–40 mL of drug and are refilled through a catheter access port. They also need to be surgically replaced every 4–7 years based on battery life.[24] Miniaturized, soft devices capable of providing localized, on-demand drug delivery could substantially improve care of patients requiring ongoing pharmacologic therapy.

1.2.2. Electromagnetic Treatment

Electromagnetic stimulation has been applied to treatment of various neuropsychiatric symptoms and conditions. Devices to provide electrical stimulation can be categorized as either open-loop or closed-loop. Open-loop stimulation is applied as per a predesigned protocol that is not modified by ongoing signals from the body, while closed-loop stimulation features are determined according to feedback provided from body signals.

Open Loop: Open-loop neurostimulation technologies are commonly employed to treat chronic pain, theoretically functioning by attenuating conduction of the pain signal or increasing local inhibition.[25] Stimulators can be implanted epidurally to target the spinal cord, as well as within or on the surface of subcutaneous tissue to target peripheral nerves. Substantial evidence supports the efficacy of these approaches in treating chronic, medically refractory pain related to cancer, neuropathy, and nerve injuries.[26] Vagus nerve stimulation (VNS), accomplished by an implanted device that applies pulses of stimulation to the axons of the nerve in the neck, has widespread effects on neuronal excitability and can decrease the occurrence rate of seizures in a select group of patients with medically refractory epilepsy.[27] Similar devices can be placed over the skin to pass current over a targeted muscle or group of muscles with the goal of contracting the muscle and preventing disuse atrophy in conditions where the muscle must be immobilized, such as limb casting or hip replacement surgery.[28]

Noninvasive stimulation of the brain can be accomplished using either electrical or magnetic stimulation, with devices placed on the scalp over the brain region of interest during the epoch of treatment. Although the mechanisms underlying these stimulation approaches are incompletely understood, they are thought to activate or inhibit action potential generation depending on the parameters of stimulation applied.[29] Transcranial electrical stimulation (TES) is considered investigational for all purposes, but studies of its efficacy are ongoing for medical conditions including headaches, pain, insomnia, anxiety, and substance abuse treatment.[30] Transcranial magnetic stimulation is also under investigation for many of these disorders, but has only been approved for treatment of refractory major depressive disorder[31] (NeuroStar TMS Therapy System) and obsessive-compulsive disorder[32] (BrainsWay Deep TMS). Many studies employing TES and TMS have low numbers of subjects as well as heterogeneous technologies and protocols.

Deep brain stimulation (DBS) is an invasive approach that involves chronic implantation of a device that delivers electrical pulses to specific brain areas. Such devices are comprised of a pulse generator, usually implanted near the clavicle or in the abdomen, that is connected by subcutaneous wiring to leads that are inserted into the brain. The pulse generator can be programmed to deliver continuous or diurnally varying stimulation. Most conventional DBS systems use cylindrical electrodes that deliver omnidirectional stimulation and therefore affect neurons around the circumference of the electrode. More recently, directional electrodes have been developed in

an attempt to minimize side effects caused by stimulation of off-target brain areas[33] (St. Jude Medical Infinity DBS System, Vercise DBS System). DBS that targets the basal ganglia, a key center for motor control, results in clinically significant reduction in symptoms for patients with Parkinson's disease, essential tremor, and primary dystonia.[34–36] Studies are ongoing for patients with epilepsy, multiple sclerosis, treatment resistant depression, obsessive-compulsive disorder, Tourette's syndrome, and even drug addiction, but there is currently insufficient evidence for widespread clinical use.

In all cases, materials and devices that improve the efficacy of stimulation, decrease the cost per subject, minimize side effects, and simplify routine use of the technology would be expected to improve the quality of clinical studies and perhaps expand the applicability of these approaches to a broader range of disorders.

Closed Loop: Closed-loop stimulation therapies have the advantage of providing treatment only when a biomarker of neurologic disease is detected. This type of approach potentially improves the efficacy of several open-loop interventions and decreases associated side effects.[37]

For instance, when the spinal cord stimulation parameters are tuned based on body posture information that is acquired by an accelerometer, patients with intractable neuropathic pain often experience improved pain relief.[38] Closed-loop vagal nerve stimulation (AspireSR) triggered by increases in heart rate associated with seizures is approved for clinical use, and may improve efficacy over conventional VNS in selected patients.[39] Automated triggering of DBS based on brain signals recorded from the basal ganglia in patients with Parkinson's disease (Activa, Medtronics PC+S neurostimulator) may also improve outcomes and increase device battery life.[40] Closed-loop therapy used to abort seizures based on intracranial detection of electrophysiologic seizure patterns (NeuroPace) has demonstrated clinical safety and efficacy in reduction of seizure frequency in selected patient populations, in contrast to open-loop approaches that have been mostly ineffective.[41,42] Therefore, the ability to transform open- to closed-loop therapies holds promise for better patient outcomes. However, this process is beset by challenges related to accurate sensing of relevant biomarkers and implantation of electronic components capable of performing signal processing, most of which are nonbiocompatible and therefore require strong encapsulation in physiological environments.

Substantial effort is also dedicated to devices aimed at facilitating patient movement rather than controlling neurologic symptoms. For many patients who have lost mobility due to injury of the limbs or spinal cord, amyotrophic lateral sclerosis, or brainstem stroke, closed-loop devices offer the possibility of restoring independence and improving quality of life. Here, electronics are interfaced with either the central or peripheral nervous system to translate movement intent into physical manifestation. Noninvasive approaches involve the use of microcomputer-controlled electrical pulses applied through electrodes placed on the skin over targeted nerves and muscles. For example, devices have been developed that assist gait abnormality due to dysfunction of a peripheral nerve in the leg by sensing onset of gait using a sensor worn in the shoe, triggering cutaneous nerve stimulation to increase dorsiflexion through a cuff worn below the knee (WalkAide, Bioness NESS L300). The Parastep ambulation system uses a similar approach to initiate a sequence of muscle contractions in the lower extremities that enable a patient with lower spinal cord injury to stand, sit, and take steps. Prostheses can also be integrated with functioning nerves or muscles in patients with limb amputations to restore distal motor function of the extremity.[43] To enable a greater diversity of controllable movements in patients with brain or spinal cord diseases, high spatiotemporal resolution brain signals are required, necessitating invasive implantation of devices into brain tissue. Typically, microelectrode arrays (96 channels, Blackrock Microsystems)[44] have been implanted into motor or parietal cortex, with acquired signals used to control a variety of effectors, from a keyboard to robotic limb (LUKE arm, modular prosthetic limb)[45] or exoskeleton (CLINATEC BCI platform).[46] These systems encounter challenges in maintaining consistent, chronic recording of the brain signals required to operate the devices, require intensive training before effective use begins, and are difficult to operate outside of a clinical environment (e.g., in the home). Furthermore, the devices are currently unable to integrate sensory feedback, which is crucial for tuning and adjustment of motor movements.

As our understanding of the nervous system and its pathophysiology progress, potential applications for bioelectronic devices to diagnose and treat neuropsychiatric diseases are increasingly hypothesized. However, appropriate clinical testing of these hypotheses requires new approaches to the material design of bioelectronic devices to optimize efficacy and minimize potential risks. Here, we address each main component of bioelectronic devices and discuss advances that could improve translation to clinical use.

1.3. Clinical Development

The Food and Drug Administration (FDA) provides documentation outlining approval requirements for neurological devices. The basic process of neural device development for clinical use involves formalizing the device design and fabrication, establishing sterilization protocols, completing Institutional Review Board (IRB) approval at investigators' institutions (where the device is to be tested or used outside of FDA oversight), and ultimately acquiring FDA approval. Medical devices require stringent testing before commercialization, which is governed by the Center for Devices and Radiological Health (CDRH) within the FDA. Further, neurotechnology devices are primarily reviewed by the Division of Neurological and Physical Medicine Devices (DNPMD).[47] The process of registering a medical device involves regulation commensurate with risk associated with device use, classified as Class I, II, or III in order of escalating risk. Class I devices are often simple in design and have minimal potential risk to the patient. Very few neurological devices hold this classification, though ventricular needles and anvils used to form skull plates fall in this category.[48] Noninvasive neurological devices such as biofeedback and diagnostic EEG sensors and some invasive devices such as neurostimulators fall under Class II devices because they require regulation beyond general controls. These special controls include labelling requirements, performance standards, and postmarket

surveillance. Finally, devices that are implanted or life-sustaining fall under Class III, such as deep brain stimulators. These devices involve general controls and premarket approval activities that include clinical trials. The regulations that are associated with each class of device assure safety and effectiveness and are governed by Code of Federal Regulations (CFR) Title 21 for general device types and 21 CFR Part 882 and 890 for neurological and physical medicine devices, respectively.

2. Functional Pillars of Neuroelectronics

2.1. Acquisition Materials and Devices

The overall goal of acquiring neural signals is to be able to decode the neural syntax, detect dysfunction, and correct or even prevent this dysfunction. Complicating this goal is the fact that information is processed in the brain at different spatial and temporal resolutions. On the millisecond time scale, an action potential is the unit of communication between individual neurons. Action potentials are generated when a sufficient number of neurotransmitter-gated ion channels within the neuronal cell membrane are opened, resulting in a large change in the electric potential across the membrane in a spatially restricted region. This ion-mediated electrical potential becomes self-sustaining and propagates down the neuron's axon due to activation of adjacent voltage-gated ion channels. Action potentials induce neurotransmitter release at the neuron's presynaptic terminal, allowing communication with the postsynaptic neuron. The changes in ionic flux that result from action potentials can be detected using extracellular electrodes with sizes similar to the neuronal cell body at micrometer scale distances from the neuron. Similarly, changes in ionic flux that result from the opening of postsynaptic ion channels in a population of neurons can be detected as the local field potential (LFP).[2,49] This synaptic activity is often in the form of brain oscillations at defined frequency bands, and is a result of interactions between excitatory and inhibitory neurons within microcircuits. These brain oscillations have a wide range of frequencies (a few milli-Hertz to several hundred Hertz) and are known to organize sequences of action potentials, establish communication between brain regions, play a causal role in several behavioral functions, and are used as biomarkers for various neurological conditions. Therefore, an ideal neural interface device would be able to acquire action potentials and LFP with high spatial and temporal resolution across large area of the brain simultaneously. The electrode size and material are key parameters that define the spatial and temporal resolution of the acquired signal at a given location, whereas the density and geometrical distribution of the electrodes define the spatial scale of the recordings.

2.1.1. Materials at the Interface with Neural Tissue

The electric fields generated by nervous tissue are the result of ion movement. The efficiency of an electrode in converting ionic signals into electronic ones can be quantitively evaluated by the electrochemical impedance spectrum of the electrode across a physiologically relevant frequency band (0.1 Hz to 10 kHz). Typically, the electrochemical impedance of an extracellular electrode is reported at 1 kHz, which reflects the corresponding frequency of an action potential period (1 ms). The effective surface area of the electrode and the electrode material are the two key parameters defining this impedance value through the capacitance formed between the electrode and ions in the electrolyte, known as electric double layer capacitance.[50] The larger the electrode surface area, the larger the area of double layer electrical capacitance between electrolyte and the electrode, hence the lower the impedance. However, large electrodes will result in more spatially summated neural activity, limiting the spatiotemporal resolution of the electrode. Therefore, the optimal electrode size is defined by a trade-off between required resolution and electrochemical impedance of the electrode. For example, to be able to acquire an individual neuron's action potentials, the electrode size should be close to the size of the neuron's cell body and spaced to match the density of neurons within the tissue. This restricts the upper band of electrode geometry to ≈10–20 µm in the majority of brain regions, although denser regions with smaller neurons may require smaller electrodes, and similarly, larger electrodes may be used in areas with larger and less closely packed neurons.

Electrode material and its electrochemical properties define the capacitance value of the interface, and this capacitance is inversely related to the overall impedance of the electrode. In general, the neural electrode materials can be categorized as either polarizable or nonpolarizable based on their faradaic interactions with electrolyte. Although nonpolarizable electrode materials, such as Ag/AgCl, that can pass current across electrolyte-electrode interface with minimal resistance are preferred, the deposition of metal ions (such as AgCl) in vivo poses major biocompatibility concerns and precludes their use in high density implantable devices. These materials are often embedded into hydrogels that serve as ion-conductive physical barriers in noninvasive EEG, electrocardiography (ECG), and electrooculogram (EOG) electrodes. On the, other hand, polarizable, chemically stable metals such as Au, Pt and stainless-steel have been extensively used as in vivo implantable electrode materials in both research and clinical applications. Several approaches have been employed to improve their capacitance and charge capacity, typically by increasing the electrode's effective surface area while maintaining the overall macroscopic geometry of the electrode.[51] These strategies include nanoscale surface patterning, deposition of the electrode material on rough surfaces, use of nanoparticles to form complex 3D nanostructures, and electrodeposition protocols with enhanced surface roughness. A prime example of this strategy is generation of platinum black, which has substantially larger surface area than conventional Pt. In addition to nanoscale enlargement of surface area, metal oxides and nitrides such as Ir/iridium oxide and TiN can further increase the charge capacity of the interface and have been used in several high-density neural interface devices (**Figure 2**A–C).[52–57]

In parallel to metal-based electrodes,[58–60] conducting polymers (a class of organic electronic materials) have gained substantial attention as an electrode coating material that improves the impedance of neural electrodes. Among these materials, the conducting polymer poly(3,4-ethylenedioxythiophene)–poly(styrenesulfonate) (PEDOT:PSS) has been highly used

in a large variety of applications and scales due to its commercial availability, high conduction, and stability in physiological environments.[61–63] Originally, Martin et al. introduced PEDOT:PSS as polymer electrode coating for implantable silicon probes (Figure 2D,E). They used an electropolymerization technique to coat the existing metallic surface of silicon-based neural probe electrodes with PEDOT:PSS. Signal-to-noise ratio (SNR) and long-term stability in vivo was improved for chronically implanted PEDOT:PSS-based electrodes compared to conventional metal electrodes.[64–66] The simplicity and highly

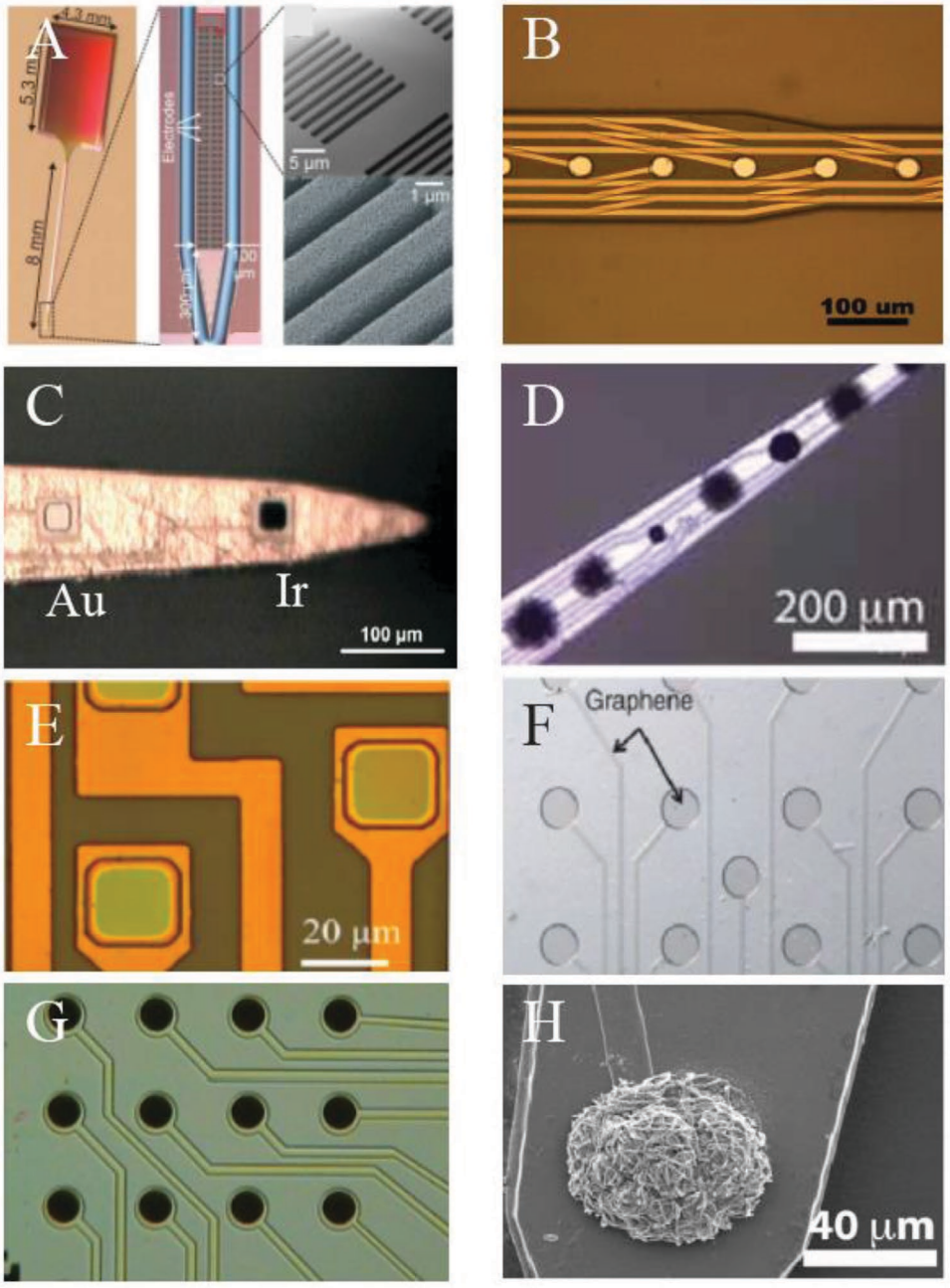

Figure 2. Neural interface electrode materials. A) TiN electrode used in a Neuropixel probe. Reproduced with permission.[232] Copyright 2018, Elsevier. B) Microscopy image demonstrating crossover of two metal sandwich layers (Ti/Pt/Ti) and exposed platinum electrode sites. Reproduced with permission.[182] Copyright 2008, Elsevier. C) Optical images of gold and Ir-plated electrode sites before the pulse test experiment. Reproduced with permission.[233] Copyright 2011, Elsevier. D) Electrochemical deposition of conducting polymer (PEDOT) on electrode sites and around electrospun PLLA nanofiber templates. Reproduced with permission.[234] Copyright 2010, Wiley-VCH. E) Photolithographically patterned conducting polymer electrodes. Reproduced with permission.[235] Copyright 2011, Wiley-VCH. F) High-magnification image of a surface array with transparent graphene electrode sites. Reproduced with permission.[220] G) Optical micrograph of a multielectrode array device made with carbon-nanotube-based pillars. Reproduced with permission.[236] Copyright 1991, Royal Society of Chemistry. H) SEM image of PPy nanotube outgrowth on silicon dioxide showing diameter outgrowth of 60 µm. Reproduced with permission.[234] Copyright 2010, Wiley-VCH.

reliable electro-polymerization process for PEDOT:PSS was successfully deployed in several laboratories and industrial sectors as part of the electrode fabrication process.

While effective, the electrodeposition process of conducting polymers still poses two major challenges: i) the electrodeposition is limited to conducting surfaces and cannot be used to selectively coat nonconducting surfaces, and ii) the stability and adhesion of the conducting polymer is highly sensitive to deposition protocols and use of crosslinking agents is limited. To overcome these challenges, orthogonal photoresists combined with dry etching processes can be used to perform photolithographic patterning of PEDOT:PSS at high resolutions.[67,68] This process allows modification of commercially available dispersions to achieve highly conducting patterned PEDOT:PSS. However, addition of crosslinking agents such as GOPS substantially slows the plasma etching process and limits the tractable thickness of the patterned polymer using this method. Instead, a photolithographic process involving patterning and delamination of an inert sacrificial layer acting as a micropattern shadow mask can be used with many relevant polymers, including modified PEDOT:PSS, on a variety of surfaces (Figure 2E).[69,70]

Beyond demonstrating improved impedances, organic material-based electrodes offer other unique advantages, including transparency (Figure 2F)[71] and higher surface areas (Figure 2G,H). Conductive polymer coated electrodes also demonstrate the ability to absorb and release biomolecules through swelling. For example, Cui et al. were able to successfully "load" graphene-based electrodes coated with an electrodeposited polymer film with anti-inflammatory drugs prior to insertion in the brain. After implantation, the hydrophilic nature of the polymer resulted in uptake of water and exchange of the drug with the surrounding tissue.[72]

2.1.2. Signal Amplification, Multiplexing, and Processing

To obtain high-quality, multichannel neural recordings, signal amplification, multiplexing, and processing must be performed. Neural signal amplification is accomplished via biopotential amplifiers, which must amplify signals with high gain and low noise. Given that the external sources of interference (such as myoelectric potentials from muscle contractions, 50 or 60 Hz AC power, or environmental radio frequency signals) can be several orders of magnitudes larger than neural signals, recordings are performed using a differential setup. Such a setup requires grounding the subject, and performing recordings using at least two electrodes—one to record neural activity, and the other to serve as a reference. The interfering noise then appears as the common-mode signal to a differential amplifier, which if ideal (i.e., with infinite common-mode rejection ratio (CMRR), infinite input impedance, and zero electrode impedance) would completely suppress that common-mode signal. Typical neural amplifiers display CMRRs in the range of 70–120 dB.[73]

Because sampling each neural waveform to a distinct line would require an equal number of leads as electrodes and limit number of electrodes that could be used, multiplexing is applied to combine several amplified signal lines into one data line.[74–79] In time division multiplexing (TDM), the multiplexer selects and forwards one slice of each line to its output line for a given time interval (the sampling window); by switching through all inputs, the multiplexer samples multiple channels into a single line. In turn, at the receiver a demultiplexer enables reconstruction of individual input signals from the multiplexed line.

In addition to multiplexing, neural acquisition systems must also digitize the amplified and multiplexed signal, a task accomplished by analog-to-digital converters (ADCs). This conversion usually occurs after multiplexing to reduce the total number of required ADC lines. In order to satisfy the Nyquist–Shannon sampling theorem (and enable perfect reconstruction of the continuous data from the discrete data), these converters must operate at a sampling rate greater than twice the bandwidth of the signal of interest.[80]

This section describes different approaches to amplifying, multiplexing, and processing signals for neural recordings, according to employed transistor material type.

Silicon Transistor-Based Devices: Silicon-transistor based devices incorporate amplification, multiplexing, and/or processing capacities into integrated-circuits or, more recently, flexible arrays. Silicon-based integrated-circuits are packaged, often implantable chips that receive neural signals from tissue-interfacing electrodes or probes as inputs, and yield amplified, multiplexed, and potentially further filtered signals as outputs. The first monolithic, microprocessor-based telemetry system for neurophysiological recordings, developed in 1985, was based on a micropower signal processor capable of amplifying, filtering, and multiplexing three neural action-potential waveforms detected by microwire electrodes.[81] While that chip interfaced with wire electrodes, ICs can also interface with silicon-based probes, like the Utah array (**Figure 3**A) or the Michigan probe (Figure 3B).

IC-incorporating implantable probes have also been developed. The first probe, developed in 1986, included ten recording electrodes and corresponding on-chip electronics, namely, one preamplifier per electrode, an 11:1 multiplexer (driven by an 11-stage two-phase dynamic shift register), power-on-reset circuitry, and high-speed, unity-gain broad-band output buffer.[82] Further, the later-developed "Neuropixel" probe is comprised of a tissue-interfacing shank (tiled by low-impedance TiN sites) and base (on which voltage signals could be filtered, amplified, multiplexed, and digitized) for noise-free transmission of digital data (Figure 3C).[52] Digital signals are more resistant to noise interference, and can be protected from data corruption with a cyclic redundancy code (CRC) checksum. Therefore, such on-chip digitization, which was also employed by Muller et al.[83] in creating a 26 400 microelectrode array, allowed for more robust data to be transmitted off-chip.

Multiplexed silicon-based neural interface arrays have also been developed (Figure 3D,E). Fang et al. produced a flexible array consisting of capacitive sensing nodes, whereby each node consisted of an NMOS source-follower amplifier with a capacitive input, and on-site NMOS multiplexer.[79,84] This array was covered by an ultrathin, thermally-grown layer of SiO_2, to act as a dielectric and enable capacitive coupling, as well as acting as a barrier to prevent penetration of biofluids (Figure 3F).[85]

Organic Transistor-Based Devices: Because silicon-based circuitry requires encapsulation in physiological environments, chronic, fully-implantable silicon-based devices are often bulky and display limited channel count and processing capabilities. Since biocompatible organic electronic materials can perform

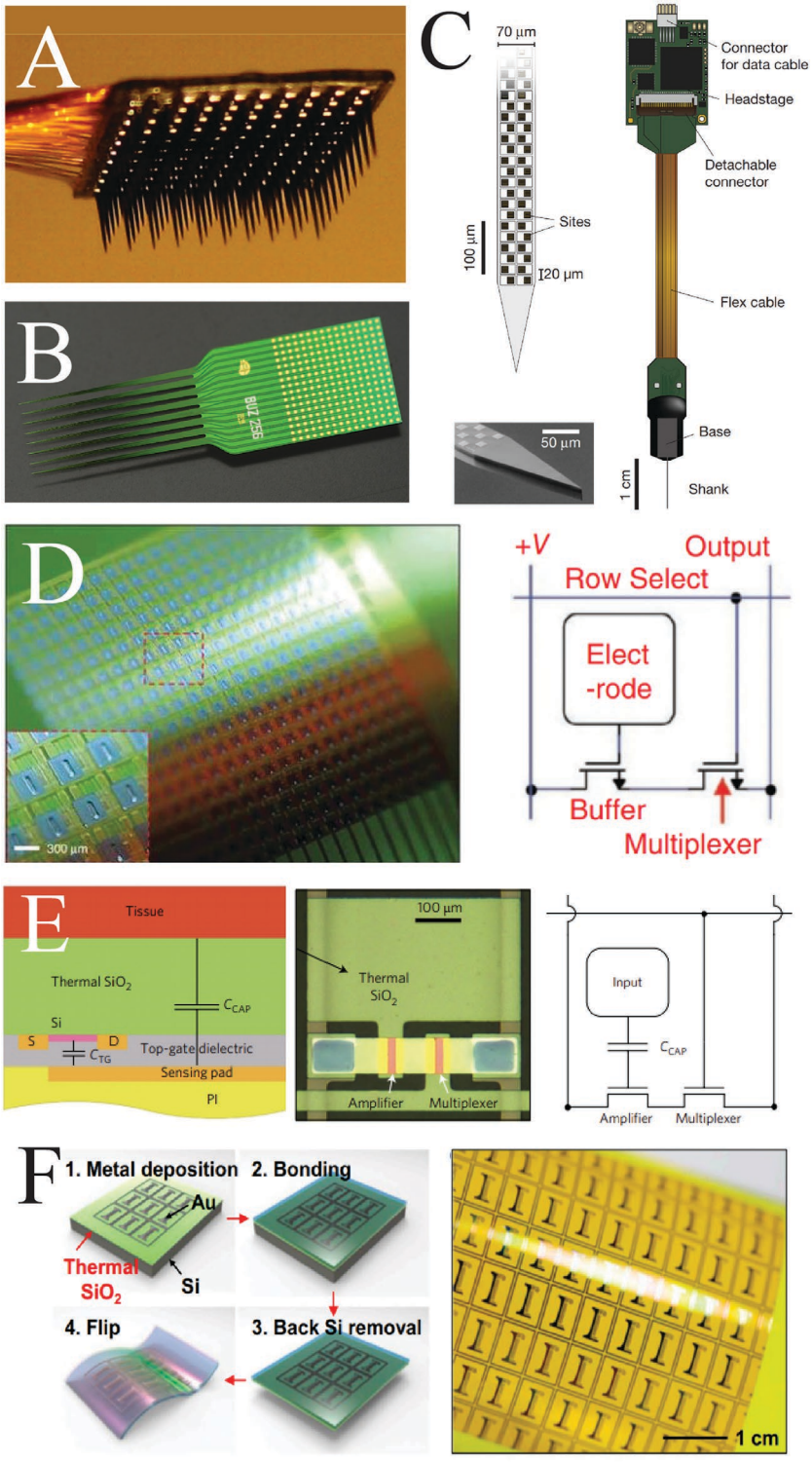

Figure 3. Silicon-based neural interface devices. A) A 10 by 10 Utah array. Reproduced with permission.[255] Copyright 2007, Society for Neuroscience. B) The Michigan probe, also known as an Si-probe. The image is of an 8-shank, 256-channel probe manufactured by NeuroNexus. Reproduced with permission. Image courtesy of NeuroNexus, Ann Arbor, USA. C) Probe tip (left) and packaging (right) of Neuropixel probe capable of recording of 384 channels simultaneously. Reproduced with permission.[52] Copyright 2017, Springer Nature. D) Flexible Si-based transistor used in a surface array to perform local buffering and multiplexing. Reproduced with permission.[79] Copyright 2011, Springer Nature. E) Capacitively coupled silicon nanomembrane transistor as an amplified sensing node. Circuit diagram (left) and optical microscopy image (middle) of a node. Mechanism for capacitively coupled sensing through a thermal SiO_2 layer (right). Reproduced with permission.[84] Copyright 2017, Springer Nature. F) Steps to thermally grow, transfer, and integrate ultrathin layers of encapsulating SiO_2 onto flexible electronic platforms (left). Sample with 100 nm thick layer of thermal SiO_2 on top surface (right). Reproduced with permission.[85] Copyright 2016, National Academy of Sciences.

local amplification when used within transistor architectures, organic transistor-based devices have been explored for local amplification of neural signals.

Multiple organic transistor architectures have been applied for neural recordings. In the solution-gated field-effect transistor (SGFET, which is a type of electrolyte-gated OFET (EGOFET)) an organic semiconductor film connects the source and drain electrodes, and a liquid electrolyte separates the channel from the gate electrode.[86–88] Given their electrolyte-gating, SGFETs are well-suited to biosensing. Hess et al. used arrays of graphene SGFETs to detect action potentials from electrogenic cells (cardiomyocyte-like HL-1 cells).[89] Hebert et al. demonstrated that when taking recordings from the surface of the cortex, graphene SGFETs exhibit a similar SNR below 100 Hz as platinum black electrodes do, but cannot record signals above 1 kHz. They also successfully recorded slow-wave activity, synchronous activity, and potentials on the auditory and visual cortices.[90] Masvidal-Codina et al. further showed that graphene SGFETs arrays can be used to record a wide bandwidth of neural signals, ranging from infraslow frequencies (<0.1 Hz) to typical local field potential bandwidth (**Figure 4**A).[91] Cisneros-Fernandez et al. also established a scheme to enable large-scale µECoG recordings with SGFETs, via frequency-domain multiplexing (FDM). Their approach, involving use of SGFETs both as transconductance amplifiers and voltage mixers (with voltage mixing occurring a column voltage carrier and an µECoG signal), allows hybrid integration of SGFET arrays and read-out ICs.[78]

The organic electrochemical transistor (OECT) has also been widely used for bio-signal transduction. In the OECT, an electronic channel formed by patterning a conducting polymer between two electrodes is (de)-doped by injection of ions from an electrolyte. Conformable arrays of OECTs were therefore shown to enable the recording of brain activity, such as low-amplitude brain signals at the somatosensory cortex of rats[92] (Figure 4B,C). While capable of transducing such signals, OECTs, having transient characteristics that are controlled by the time needed for ions to travel between the electrolyte and polymeric channel, display slow switching speeds. To overcome this limitation, internal ion-gated organic electrochemical transistors (IGTs) embed mobile ions in the conducting polymer defining the transistor channel. This design enables faster response times ($\tau = 2.6$ µs) than observed in OECTs, for which the transient response is characterized by both the time constants for ionic transport in electrolyte (τ_i) and electronic transport (τ_e).[93] Spyropoulos et al showed that IGTs fabricated into a conformable ribbon structure could be applied to human EEG; their "µ-EEG IGTs" adhered directly to skin without additional chemicals, and enabled capture of alpha, beta, and low-gamma oscillations (Figure 4D).[94] In the same direction, Cea et al. developed conformable, implantable, enhancement mode IGTs for in vivo recording of neural action potentials, and circuitry for real-time detection of epileptic discharges[95] (Figure 4E).

2.2. Stimulation Materials and Devices

Neural stimulation enables modulation of brain activity, both for the purposes of understanding function of neural networks and treating dysfunction of these networks. In this section we

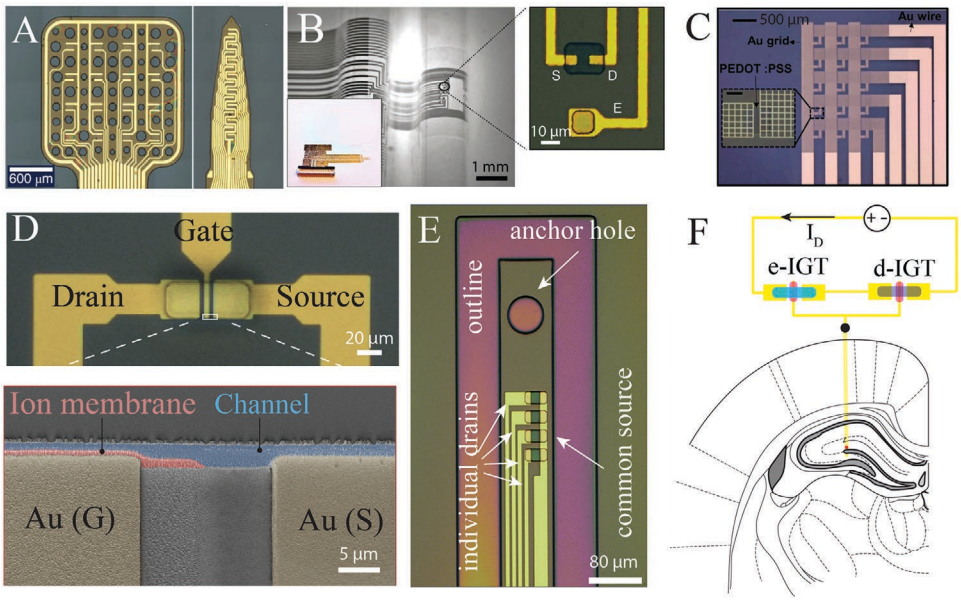

Figure 4. Materials and architectures of transistors used in neuroelectronics. A) Graphene-based transistors for surface and depth recordings. Reproduced with permission.[91] Copyright 2018, Springer Nature. B) OECT-based ECoG array, with inset showing an optical microscopy image of an OECT and adjacent conducting polymer electrode. Adapted with permission.[92] Copyright 2013, Springer Nature. C) An OECT-based surface array with mesh-like Au interconnects for optical transparency. Reproduced with permission.[237] Copyright 2017, National Academy of Sciences. D) Top view of an IGT (top), with cross-section SEM image of an IGT between gate and source electrodes (bottom). Reproduced with permission.[94] Copyright 2019, AAAS. E) Optical micrograph of an e-IGT-based device with 4 transistors for LFP and spike recording (left). The anchor hole facilitates insertion of the conformable device into deep layers of rat cortex. The potential generated by neurons serves as the small-signal V_G. Reproduced with permission.[95] Copyright 2020, Springer Nature. F) Circuit diagram of two complementary IGTs used to record real-time detection in the rat hippocampus. The rat brain coronal slice schematic has the recording site indicated (red dot). Reproduced with permission.[95] Copyright 2020, Springer Nature.

aim to provide an overview of various stimulation methods based on their primary source of stimulation energy.

2.2.1. Electrical Stimulation

Materials: Electrical stimulation involves applying a constant or alternating pattern of voltage or current to the brain (intercranial) or scalp (transcranial) tissue. Noninvasive types of electrical stimulation, like transcranial (TES), are based on the use of skin-interfacing electrodes fabricated from metals, elastic carbon, hydrogels, and conducting polymers. Conventionally, metal electrodes have been used in both invasive and noninvasive stimulation procedures.

To ensure biocompatibility, electrodes are typically made from inert materials such stainless steel, Au, or Pt. A key defining factor in efficient delivery of charge from electrode to tissue is reliable electrode-skin contact through an interface providing the largest area possible, while ensuring homogeneous current density across the electrode. To improve metal electrodes' interface and mechanical stability with biological tissue, such electrodes are often coupled with an ion-conducting adhesive gel (or historically, covered with salt water saturated fabrics). In this setup, the electric current transforms into ionic current at the metal–electrolyte junction.[96] However, the rigidity of metal electrodes combined with their polarizable electrochemical characteristics, renders them nonideal for interaction with tissues. Hydrogel-based electrodes have replaced metal electrodes in many applications. Self-adhesive electrodes for transcutaneous stimulation can consist of two hydrogel layers: a base, conductive-gel layer made from polymerization-derived copolymers, like acrylic acid and *N*-vinylpyrrolidone, and another connecting the first layer to the conductive substrate such as carbon rubber, carbon film, or wire mesh. A scrim layer can also be incorporated between the two hydrogel layers to prevent slippage, or redistribute the stimulation current[96] (**Figure 5**A). Similar to strategies employed for recording electrodes, conducting polymer-based hydrogels have been used for transcranial as well as intercranial stimulation due to their large volumetric capacitance and mixed ionic and electronic conduction (Figure 5B).[61,97–102]

Invasive electrical stimulation devices such as deep brain stimulation (DBS) electrodes usually incorporate smaller electrodes than those seen in noninvasive devices, are made out of inert material metals (e.g., platinum or platinum–iridium), and are inserted into the brain tissue to provide more local neural stimulation. DBS devices make use of unsegmented or segmented metal (e.g., platinum or platinum–iridium) electrodes (Figure 5C).[103] Retinal ganglion cell stimulation has been accomplished using "brush-like electrodes" formed from parylene-C coated, wet-spun liquid crystal graphene oxide (LCGO) fibers via laser ablation; implantation of these continuous, free-standing flexible probes was enabled by encapsulating them in a water-soluble sugar microneedle, which could be inserted into the tissue (Figure 5D).[59] Stimulation via transistors, rather than passive electrodes, has also been performed. Williamson et al. demonstrated that flexible, OECT-based depth probes could be implanted by aid of SU-8 shuttles (from which the probes delaminated after insertion). Application of monophasic current pulses to CA3 area of rat hippocampus pyramidal cell layer through OECTs was shown to be sufficient to evoke network and single cell responses (Figure 5E).[104]

Implantable arrays of electrodes have also been employed to achieve electrical stimulation. Liu et al. demonstrated that a thin-film elastic array of micropatterned electrically conductive hydrogel (MECH) electrodes could conformably wrap around the sciatic nerves of mice to stimulate muscle movements at low voltages (50 mV). This hydrogel was based on the conducting polymer PEDOT:PSS, and demonstrated an electrical conductivity of 47.4 ± 1.2 S cm^{-1}, as well as current density (under a bipolar pulsed voltage of 0.5 V at 50 Hz) that was orders of magnitude higher than that of electrodes made by a pure ionic conductor (Dulbecco's modified Eagle's media) or platinum electrodes (Figure 5F).[99]

Systems: Electrical stimulation involves applying a constant or alternating pattern of voltage or current to the brain (intracranial) or scalp (transcranial) tissue.

Traditionally, this has been performed in the form of an open-loop stimulation. However, closed-loop electrical stimulation has gained significant attention recently, and is being investigated for various neuropsychiatric disorders. Liu et al. demonstrated a fully-programmable, bidirectional neural interface system capable of i) acquiring 16-channel, low-noise neural amplifiers (based on 180 nm CMOS technology), ii) extracting neural waveform features, and iii) performing closed-loop electrical stimulation of neural circuits based on proportional-integral-derivative (PID) controllers (Figure 5G).[105] Whereas that system realized the closed-loop control on each channel through PID controllers, field-programmable gate arrays (FPGAs) have also been utilized to provide required computation for processing the ongoing feedback signal and controlling the stimulating circuitry. Zhou et al. develop a 128-channel, wireless neuromodulation device (WAND) that used an FPGA to run closed-loop algorithms, cancel residual artifacts (i.e., the large voltage transients resulting from stimulation), and detect neural biomarkers based on their waveform characteristics.[106] Park et al. employed an FPGA to develop a closed-loop, 128-channel spike-sorting system, which is the process of assigning neural spikes to an individual neuron (unit) for real time clustering of neural spikes into putative individual neurons.[107] Seu et al. used a reconfigurable FPGA-based processing system for low-latency preprocessing of spike data acquired by a 4096-electrode microelectrode array (MEA).[108]

2.2.2. Magnetic Stimulation

Magnetic stimulation, in the form of pulsed or low-radiofrequency alternating magnetic fields (100 kHz to 1 MHz), is applied for noninvasive (and to a lesser extent, invasive) excitation or inhibition of specific brain areas. Magnetic stimulation can penetrate into the body without substantial attenuation (i.e., up to the MHz range). Although this method's stimulation is typically achieved via noninvasive procedures and devices, invasive methodologies are also being explored.

Transcranial magnetic stimulation (TMS) is a noninvasive approach that relies on passing current through a coil of wire

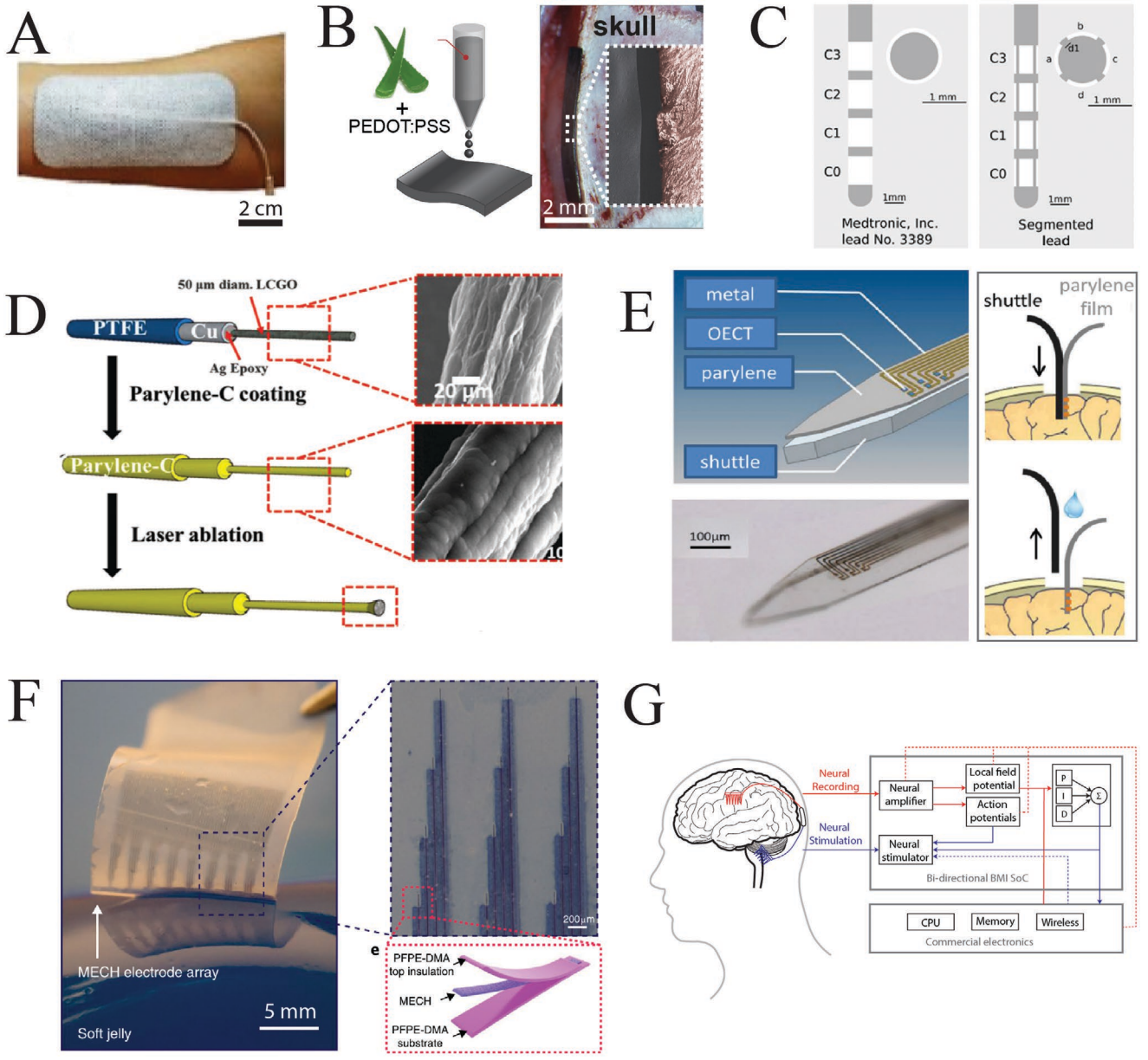

Figure 5. Electrical stimulation modalities. A) Self-adhesive electrode for transcutaneous stimulation. Reproduced with permission.[95] Copyright 2020, Springer Nature. B) Aloe vera conducting polymer film based on PEDOT:PSS and aloe vera hydrogel conforms on a rat skull (left). TES electrodes placed on the rat skull (right). Reproduced with permission.[97] Copyright 2019, Wiley-VCH. C) Unsegmented (left) versus segmented (right) deep-brain stimulation lead. Reproduced with permission.[238] D) "Brush" electrode composed of wet-spun liquid crystal graphene oxide for neural stimulation and recording. Reproduced with permission.[59] Copyright 2015, Wiley-VCH. E) Delaminating depth probes with organic electrochemical transistors penetrate the cortex and stimulate neurons. Reproduced with permission.[104] Copyright 2015, Wiley-VCH. F) Micropatterned electrically conductive hydrogel electrode array (left) consists of individual MECH electrodes (dark lines) encapsulated by fluorinated polymer PFPE-DMA (blue) (right). Reproduced with permission.[99] Copyright 2019, Springer Nature. G) Block diagram for bidirectional brain–machine interface system enabling closed-loop recording and stimulation.

(the "magnetic coil") placed above the scalp, whereby the region of stimulation can be characterized through concurrent use of electrical recording (EEG) or imaging modalities.[109] Since coil geometry changes the resultant magnetic field, magnetic coils of specific sizes and shapes, including round, figure-of-eight (F8), or Hesed (H), are employed for targeted stimulated. F8-coils are more focal, with maximal current being produced at the intersection of the two round components.[110] By contrast, H-coils, which are larger and have more complex winding patterns, are used to stimulate deeper brain structures, though with less focality.[111]

For superficial cortical regions, the spatial limits of TMS stimulation can be well-defined: TMS-induced spiking activity of single neurons in an area of the macaque parietal cortex could be confined to a 2 mm diameter region through use of a 55 mm coil.[112] However, since TMS cannot achieve specific stimulation of deeper regions, smaller, penetrating devices

have been developed. Bonmassar et al. produced micromagnetic stimulation coils that were small enough to be implanted within the brain parenchyma. Their coils were able to activate retinal ganglion cells both directly and indirectly (via activation of presynaptic neurons), with the activation respectively depending on whether neurons were near the end of the coil, or along its cylindrical length.[113] Targeted noninvasive stimulation (i.e., affecting specific subpopulations of neurons in a given brain region) can also be achieved through magnetic nanoparticles. Fe_3O_4 magnetic nanoparticles (MNPs), which dissipate heat generated by hysteresis when exposed to alternating magnetic fields, could be used to activate cells expressing the heat-sensitive capsaicin receptor TRPV1 both in vitro and in vivo. Anikeeva and colleagues observed that the transfected neurons in mice could be activated up to one month after MNP injection, with the MNP injection site exhibiting lower macrophage accumulation and glial activation as well as a higher proportion of neurons compared to a similarly size stainless steel implant one month after surgery.[114]

2.2.3. Mechanical Stimulation

Mechanical stimulation uses continuous or repeated pulses of ultrasound (US) to modulate brain activity, either by stimulating the brain directly (via transcranial focused US, or tFUS), or by enabling the passage of molecular therapeutic agents into the brain (through transiently disturbing the blood–brain barrier). A single-element FUS transducer can focus 0.5 MHz ultrasound through the human skull and generate acoustic beam profiles with lateral and axial spatial resolutions of 4.9 mm and 18.0 mm from the focal distance, respectively. Such tFUS beams can modify the amplitudes of short-latency and late-onset somatosensory evoked potentials (SEPs).[115]

Low-pressure ultrasound has also been used to stimulate genetically targeted neurons directly. Misexpression of TRP-4, the pore-forming subunit of a mechanotransduction channel in *Caenorhabditis elegans*, sensitizes neurons to ultrasound; expressing the mechanosensitive channels within the mammalian brain therefore would form the basis for cell-type or region-specific ultrasound-based manipulation of neural activity ("sonogenetics").[116] Because ultrasound can be used in conjunction with piezoelectric materials to generate direct-current output,[117] neural stimulation via US and piezoelectric nanomaterials has also been explored. Marino et al. observed high-amplitude Ca^{2+} transients after ultrasound stimulation of SH-SY5Y-derived neurons that were treated with piezoelectric tetragonal barium titanate nanoparticles (BTNPs).[118] Functionalizing BTNPs with specific molecules could then eventually enable cell-type selective, in vivo neural stimulation.

FUS has also been used to open the blood–brain barrier (BB), an anatomic barrier through which only molecules <400 Da can pass.[119] Choi et al. demonstrated the feasibility of noninvasively opening the BBB in mice (i.e., through the intact skull and skin) using a single-element FUS transducer.[120] Marquet et al. then later showed that microbubble-enhanced, FUS (ME-FUS) enables BBB opening and subsequent recovery in nonhuman primates.[119] Temporally specific opening of the BBB has potential applicability to delivery of therapeutics as well as stimulation-enabling mediators (such as virus for subsequent expression of opto- or sonogenetic proteins).

2.2.4. Optical Stimulation

Optical stimulation is based on photosensitization and activation of neurons. Photosensitivity is most commonly achieved genetically, whereby cells are made to express light-sensitive proteins that depolarize (e.g., channelrhodopsin) or hyperpolarize (e.g., halorhodopsin) neurons after exposure to different wavelengths of light (blue or yellow, listed respectively for the previous examples).[121,122] This optogenetic approach involves rapid and temporally precise control of neuronal activity in a cell-type specific manner.[123]

Silicon neural probes have been used for optogenetic applications. Schwaerzle et al. developed silicon-based neural probes with optical functionality ("optrodes") that contained platinum microelectrodes, base laser diode chips, and photographically patterned SU-8 waveguides[124] (**Figure 6**A). Yoon and colleagues designed a four-shank probe containing InGaN µLEDs and Ti/Pt/Ir recording electrodes; this probe could be used to independently control neurons localized ≈50 µm apart in the CA1 pyramidal layer of mice, and induce spikes at ultra-low optical power (≈60 nW, Figure 6B).[125] Mohanty et al. produced a reconfigurable visible-light nanophotonic platform based on waveguides defined in SiN, enabling light input from a single laser centered at 473 nm to be distributed across multiple localized emitters. They demonstrated their platform's capacities by using it to control the flow of light to an implantable nanophotonic probe containing 8 independently switchable beams, and optically activate individual ChETA-expressing Gad2 interneurons in different layers of the visual cortex and hippocampus, with sub-millisecond precision (Figure 6C).[126] Lee et al. produced a "micro-optoelectrode array" from the optically transparent wide bandgap semiconductor ZnO. This device, which was a 4 × 4 array of electrically-isolated shanks with 400 µm pitch, triggered spiking in vivo at laser power levels of about 1 µW (Figure 6D).[127] Montgomery et al. developed a fully wireless implant consisting of a PCB-based powering circuit and an attached LED; this implant, which was powered via a resonant cavity, provided sufficient light power densities and pulse characteristics for optogenetic control of mouse brain, spinal, and peripheral circuits (Figure 6E).[128]

Stretchable electronics (which apply elastic conductors as electrical interconnects between rigid or bendable active devices,[129,130] such as in a stretchable active-matrix display that used dispersed elastic conductors of single-walled nanotubes (SWNTs) in fluorinated copolymer rubber[131]) and flexible fibers are being explored for optical stimulation, too. Park et al. presented an optogenetic device that combined thin, mechanically soft neural interfaces with implantable, stretchable wireless radio power and control systems. The different form factors of this device enabled specific and reversible activation of pain circuits in freely moving, untethered mice via an integrated light emitting diode (LED) (Figure 6F).[123] Lu et al. have shown that all-polymer neural fiber probes (comprised of a polycarbonate core, cyclic olefin copolymer cladding, conductive polyethylene electrodes) exhibit low-loss light transmission, even after deformation, for optogenetic stimulation of spinal cord neural activity (Figure 6G).[132]

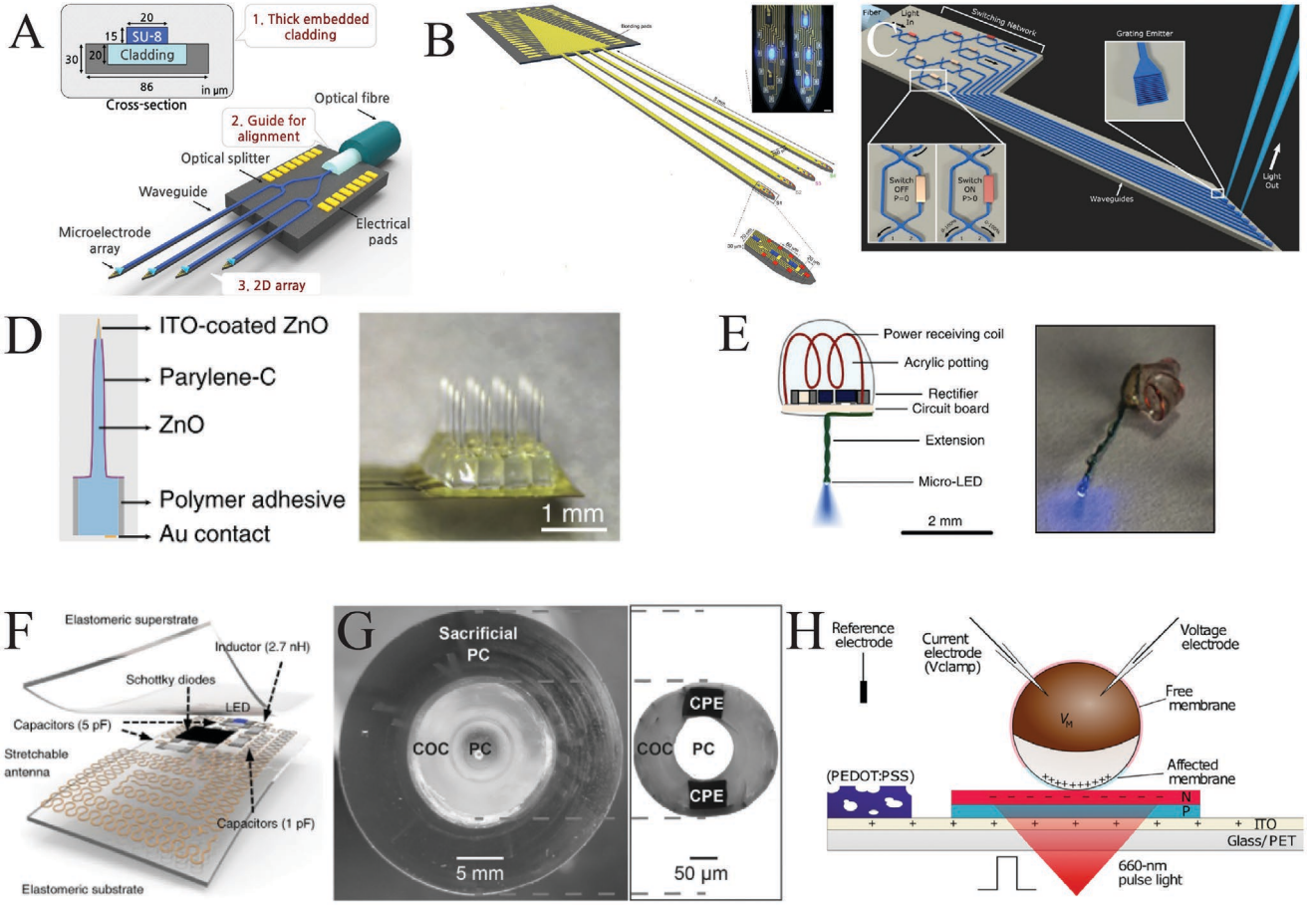

Figure 6. Optical stimulation modalities. A) Silicon-based neural probe ("optrode") monolithically integrated with SU-8 optical waveguides and microelectrode arrays. Reproduced with permission.[239] Copyright 2015, Springer Nature. B) Four-shank probe for high-resolution optogenetic manipulations. Each shank contains eight recording sites and three µLEDs. Adapted with permission.[125] Copyright 2015, Elsevier. C) Implantable silicon-based probe for optogenetic neuromodulation. Visible light entering a single waveguide is sent to a switching network, then emitted at the probe tip via grating emitters. Reproduced with permission.[126] Copyright 2020, Springer Nature. D) Micro-optoelectrode array based on optically transparent wide bandgap semiconductor ZnO. Reproduced with permission.[127] Copyright 2015, Springer Nature. E) Fully implantable wireless optogenetic device. Device is powered via a resonant cavity (not shown).[128] F) Energy harvesting unit of soft, wireless, implantable optoelectronic system. Reproduced with permission.[123] Copyright 2015, Springer Nature. G) All-polymer neural optical fiber with sacrificial polycarbonate layer. Reproduced with permission.[132] Copyright 2014, Wiley-VCH. H) Organic electrolytic photocapacitor capacitively coupling with an adjacent oocyte in electrolyte. Reproduced with permission.[137] Copyright 2019, AAAS.

Optogenetic approaches are not the only means of achieving photosensitivity in cells; cells have also been made photosensitive through nanomaterials, quantum-dots, or organic photocapacitors. Yoo et al. used near-infrared irradiated gold nanorods (GNRs) functioning as photothermal transducers bound to the plasma membrane of neurons to modulate action potentials of cultured hippocampal cells.[133] Further, Carvalho-de-Souva et al. employed gold nanoparticles (AuNPs), which are also photothermal transductors (with a plasmon absorption band peak near 523 nm) to enable optical triggering of action potentials. Since their particles were conjugated to ligands of dorsal root ganglion neuron (DRG) membrane proteins, their AuNP conjugates enabled selective binding to and stimulation of DRG neurons.[134] CdSe quantum dots have also been used to produce illumination-triggered changes in membrane potentials and ionic currents of cortical neurons in vitro.[135] Jakešová et al. recently developed organic electrolytic photocapacitors (OEPCs), which function as optoelectronic-to-ionic transducers, or light-activated external voltage-clamp electrodes. They found that when excited by short impulses of light, OEPCs produce electrolytic charging currents that can perturb the membrane potentials of nearby cells in vitro (Figure 6H).[136,137]

2.2.5. Chemical Stimulation

Chemical stimulation relies on use of pharmacological or chemogenetic methods for perturbing neural activity.[55] Delivery of chemical or biological agents can be accomplished via infusion, injection, or ingestion (**Figure 7**A). To further improve the localization and more targeted delivery can be accomplished through microfluidic, or ion pump-based neural implants. Isaksson et al. developed an electrophoretic ion pump, based on PEDOT:PSS, that functioned as actuator to pump cations (Ca^{2+}, K^{+}) from a reservoir electrolyte to a target electrolyte. This ion pump

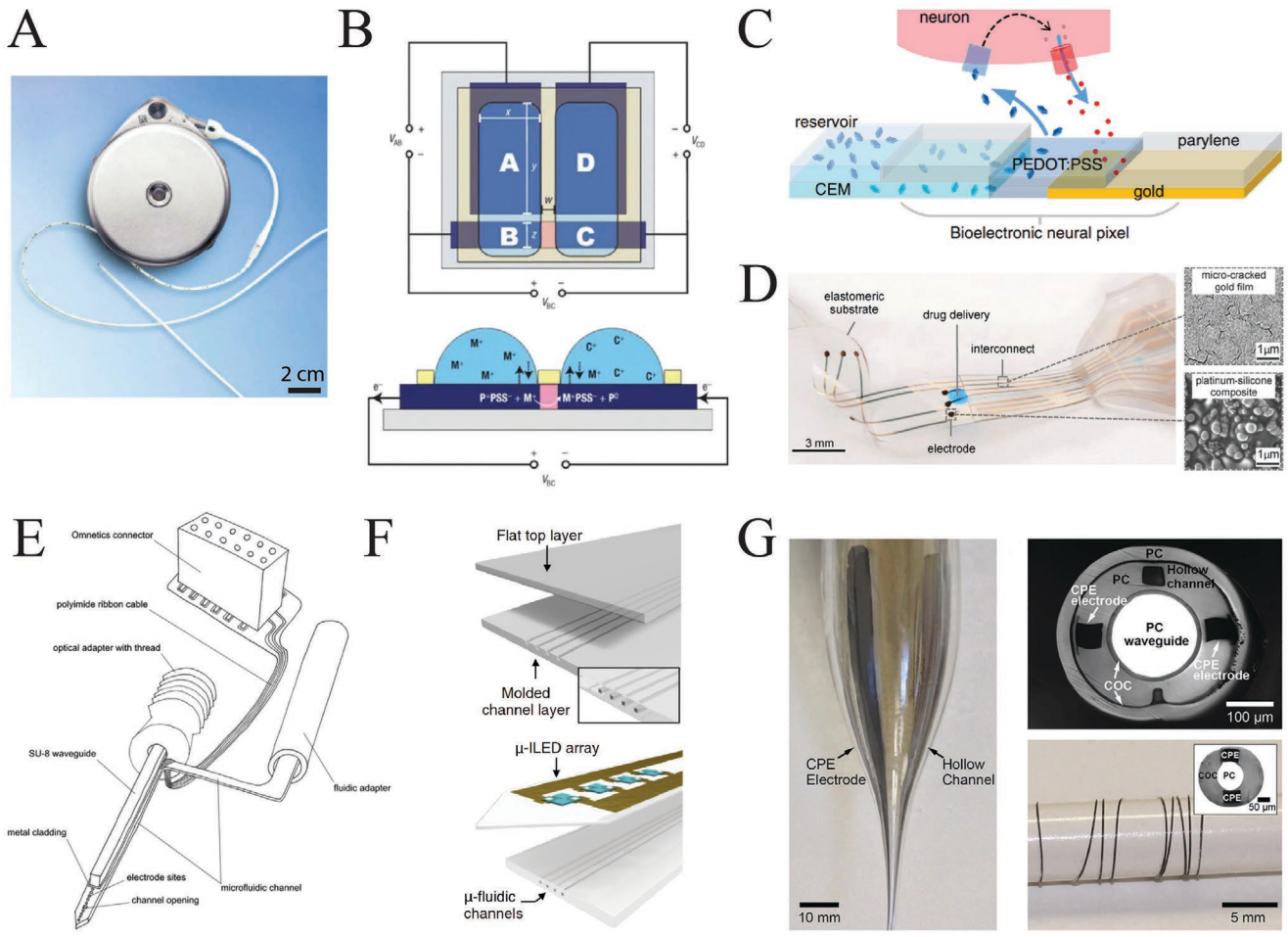

Figure 7. Chemical or multiple stimulation modalities. A) Intrathecal pump for infusion of medication into spinal fluid. Reproduced with permission.[256] Copyright 2008, Springer Nature. B) Top view (top) and cross-sectional view (bottom) of an organic electronic ion pump consisting of four PEDOT:PSS electrodes, labeled A to D. V_{BC} drives ion transport, while V_{AB} and V_{CD} regenerate B and C electrodes. Reproduced with permission.[138] Copyright 2007, Springer Nature. C) Bioelectronic neural pixel uses organic–electronic ion pumps for delivery of neurotransmitters and conducting polymer electrodes for neuronal recording. Reproduced with permission.[139] Copyright 2016, National Academy of Sciences. D) Soft neural implant with the shape and elasticity of dura mater integrating microfluidic channel for local drug delivery with interconnects and electrodes for electrical stimulation. Reproduced with permission.[142] Copyright 2015, AAAS. E) Microimplant integrating fluidic and optical simulation modalities with electrical recording capacity. Reproduced with permission.[143] Copyright 2001, Royal Society of Chemistry. F) Soft microfluidic probe integrated with a flexible array of µ-LEDs. Reproduced with permission.[144] Copyright 2015, Elsevier. G) Multimodal fiber probes combining optical stimulation, drug delivery, and neural recording capabilities. Reproduced with permission.[240] Copyright 2015, Springer Nature.

was able to stimulate individual cells, such that a cell located on a microchannel demonstrated an induced Ca^{2+} response, but distal cells did not (Figure 7B).[138] Jonsson et al. designed "neural pixels," consisting of conducting polymer electrodes for sensing and organic electrochemical ion pumps (OEIP) for drug delivery. Their neural pixel-based device could stop externally induced hippocampal epileptic activity by delivering the inhibitory neurotransmitter GABA to seizure foci (Figure 7C).[139]

Chemical stimulation can also be integrated into training paradigms. Van den Brand et al. intraperitoneally administered selected serotonin and dopamine receptor agonists to rats afflicted with paralyzing lesions prior to training the rats (via a training paradigm that relied on electrochemically enabling motor states while forcing rats to use their paralyzed hindlimbs through a robotic postural interface). This chemical stimulation and training triggered remodeling of cortical projections to restore voluntary control over locomotor movements in the rats.[140]

2.2.6. Multimodal Stimulation

The electrical and chemical stimulation modalities can be combined through use of loaded conducting polymers. The metallic electrodes of implants designed for electrical stimulation are often coated with conducting polymers (e.g., polypyrrole (PPy), poly(3,4-ethylene dioxythiophene), polyterthiophene (PTTh), etc.) to reduce each interface's electrochemical impedance. Coating the electrodes with, for example, anti-inflammatory drug or growth factor-loaded conducting polymers could therefore support tissue health around neural implants through the electro-activated elution of drugs.[141]

Microfluidic channels can also be incorporated into neural stimulation devices for delivery of multiple, distinct chemical agents. Minev et al. developed soft neural implants that transmitted electrical excitation signals (via embedded interconnects and electrodes), and delivered drugs locally (via microfluidic

channels called "chemotrodes"). Their implants integrated a silicone substrate, stretchable gold interconnects, platinum–silicone composite soft electrodes, and a silicone-embedded fluidic microchannel (Figure 7D).[142] Rubehn et al. introduced a polyimide-based implant incorporating an SU-8 based waveguide (for optical simulation) and fluidic channel (for chemical stimulation via transport of a gene delivery vector) (Figure 7E).[143] Jeong et al. generated a wireless optofluidic neural probe incorporating microfluidic channels (each of which enabled delivery of an independent fluid) and a cellular-scale inorganic micro-LED arrays (Figure 7F).[144] Canales et al. employed a thermal drawing process (TDP) to produce multimodal fiber probes that combined optical stimulation, drug delivery, and neural recording capabilities; these probes were used to record single action potentials in channelrhodopsin-expressing transgenic mice (Figure 7G).[145]

2.2.7. Conclusion

Taken together, these stimulation modalities offer possibilities for modulation of neural activity in human subjects beyond currently the clinically applied electrical and magnetic methods. Although careful testing is required to ensure safety and efficacy, it may be possible to improve the specificity of stimulation for anatomical regions and cell types. Indeed, clinical trials involving lentiviral vectors that could in the future be capable of introducing optical, ultrasonic, mechanical, and magnetic sensitivity to neurons are ongoing.

2.3. Power and Energy Devices

The variety of form-factors of neural-interfacing devices has necessitated the development of innovative means of powering such devices. Given the long history of use of batteries in contained and implantable medical devices (e.g., pacemakers), most neural interface device powering strategies have focused on use of batteries. However, batteries are chemically reactive, and require rigorous encapsulation. Form factor customization is also limited, increasing the size and weight of devices. Alternatively, energy converting approaches have been explored for powering implanted devices. For example, externally generated mechanical waves (i.e., ultrasound) can propagate through tissue to reach implanted devices containing piezoelectric materials for conversion of incident ultrasonic energy into electric charge. Furthermore, both piezoelectric and triboelectric materials (which respectively convert mechanical force into charge, or produce charge through contact electrification and electrostatic induction during frictional contact of surfaces with opposing polarities) can be applied to harvest the mechanical energy of human motion. The mechanical-to-electrical approach is therefore most applicable when a device is used in a region involving motion (e.g., on a peripheral nerve, or on the skin).

A similar approach can be employed to deliver power through transformation of electromagnetic energy. Electromagnetic waves can propagate through air to reach epidermal devices, or (though more attenuated) through tissue to reach implanted devices. Photovoltaic materials, which convert the energy of photons into energy of electrons, can be applied to power devices. Although electromagnetic waves can reach implanted devices, these waves must overcome absorption by the body and impedance mismatches (such as those existing between air, bone, and tissue) to do so. As a result, magnetic fields, which are only slightly affected by absorption or impedance mismatching, have also been exploited for powering. These external magnetic fields can be converted into local electric fields through inductive coils or magnetoelectric materials localized on the devices. This section will review the materials that enable the various approaches to powering neural-interfacing devices.

2.3.1. Chemical Energy

Both rechargeable and nonrechargeable batteries have been used within implantable devices. The implantable pulse generators (IPGs) that achieve deep brain stimulation are available in both fixed-life and rechargeable options, with their batteries lasting an average of three to five years, or 10+ years with 30 min of charging for two to three days per week, respectively.[146] The batteries of IPGs used for vagus nerve stimulation also require replacement; of the 1144 VNS procedures performed by a single surgeon between 1998 and 2012, 27% were performed due to generator battery depletion.[147] To limit battery size, implantable devices may employ step-up converters, which output a voltage higher than the input voltage. Azin et al. developed a 10.9 mm^2 intracortical microstimulation system-on-chip that employed a dc-dc converter to generate a 5.05 V power supply from a 1.5 V battery. The converter provided a maximum DC load current of 88 μA from 5.05 V to allow for an average stimulus rate of >500 Hz on each of eight channels (**Figure 8**A).[148]

2.3.2. Mechanical Energy

To enable wireless power transmission through mechanical waves, a piezoelectric crystal on the implanted device must receive and convert the mechanical energy into electricity. However, that crystal can also operate as a transmitter. Seo et al. devised a sub-millimeter implantable device involving a lead zirconate titanate (PZT) piezoelectric crystal, transistor, and a pair of recording electrodes. Because the PZT could both absorb and reflect ultrasonic energy, an external transducer could alternate between transmitting a series of pulses and listening for reflected pulses to power the device, or detecting the encoded electrophysiological signals (Figure 8B).[149]

Triboelectric materials have been applied to translate kinetic into electrical energy. Lee et al. investigated how a multilayer stack of triboelectric nanogenerators (TENGs) that produced an output voltage of 160 Vpp and short circuit current of 6.7 μA could be applied for neural stimulation. They developed sling electrodes that could be positioned around the sciatic nerve and powered with the TENG to selectively activate the tibialis anterior muscle (Figure 8C).[150]

2.3.3. Electromagnetic and Optical Energy

Electromagnetic induction has been applied to power both implantable and surface devices. Jow et al. defined a method for

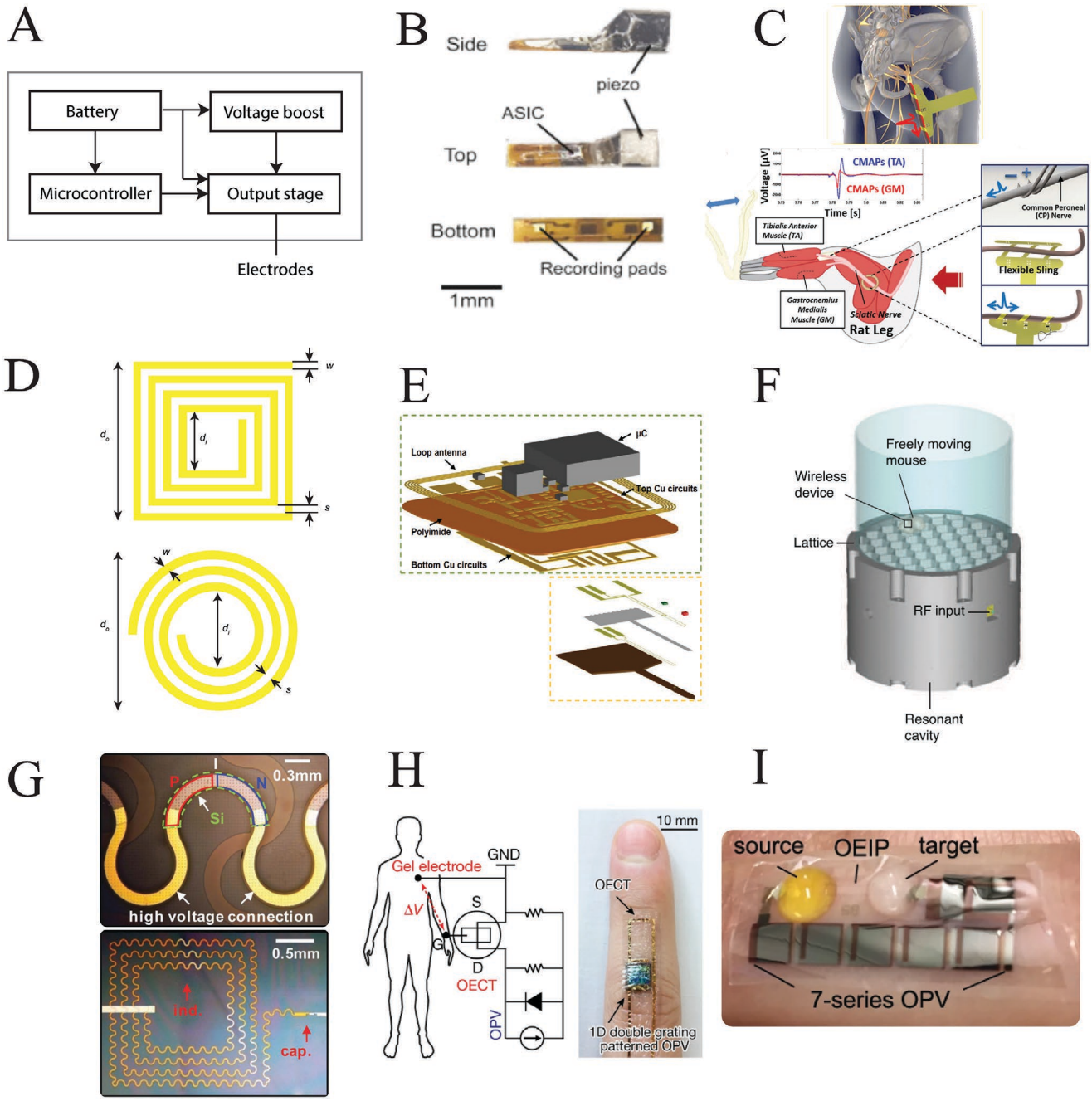

Figure 8. Power transmission strategies. A) Block diagram for typical neural stimulator. DC/DC converters boost the supply voltage to the level required by the output stage. B) Ultrasound-powered neural dust mote consists of a piezoelectric crystal, single transistor, and two recording pads. Reproduced with permission.[149] Copyright 2016, Elsevier. C) Triboelectric nanogenerator in a compressed or released state (top) generates a current (bottom). Reproduced with permission.[150] Copyright 2017, Elsevier. D) Square and circular planar spinal coils for inductive power transmission. E) Electronic (green box) and injectable modules (yellow) of a wireless oximeter. Loop antenna enables magnetic resonant coupling to an external antenna. Reproduced with permission.[152] Copyright 2019, AAAS. F) Resonant cavity for self-tracking energy transfer. Cavity is excited by a continuous-wave input. Reproduced with permission.[153] Copyright 2015, American Physical Society. G) Optical micrograph of filamentary serpentine silicon solar cell (top) and filamentary serpentine inductors and capacitors for RF operation (bottom). Reproduced with permission.[154] Copyright 2011, AAAS. H) A flexible highly stable organic solar cell as a power source for heart-rate measurements. Reproduced with permission.[241] Copyright 2018, Springer Nature. I) An organic photocapacitor is used to drive an organic ion-pump for local delivery of drug. Reproduced with permission.[155] Copyright 2019, Springer Nature.

designing printed spiral coils geometries to maximize power transmission efficiency (Figure 8D).[151] Zhang et al. used magnetic resonant coupling to power wireless, implantable optoelectronic systems for local tissue oximetry at sites of interests, including the deep brain regions of mice. Each system's power harvesting unit included a loop antenna optimized to operate at 13.56 MHz, and a half-bridge rectifier buffered by a supercapacitor. Since the output of the power harvesting unit was also

fed into a low-dropout regulator, the systems operated using a stable power supply of 3 V (Figure 8E).[152]

Ho et al. developed a resonant cavity system for wireless-powering of small-scale implants in mice (Figure 8F).[153] This system, which capitalized on the observed localization of electromagnetic energy at low gigahertz frequencies, enabled creation of implantable wireless optogenetic devices that were two orders of magnitude smaller than previously reported wireless devices.[128]

The epidermal electronics systems (EES) of Kim et al. could be powered either through induction or photovoltaic materials. Given that these systems incorporated electrodes, electronics, sensors, power supplies, and communication components into ultrathin membranes that were laminated onto the skin, material engineering techniques needed to be applied for successful integration of all components. The authors therefore developed "filamentary serpentine" (FS)-shaped components, including inductive coils and silicon photovoltaic cells, for generation of power through inductive coupling to separate transmission coils, or solar illumination, respectively. While the photovoltaic cells could generate a few tens of microwatts, generating more solar power output would have required compromising the size and mechanics of the device. Powering via inductive effects therefore was said to represent the more appealing alternative (Figure 8G).[154]

Photovoltaics have been integrated into other surface devices (Figure 8H). Jakešová et al. integrated their organic electronic ion pump (OEIP) onto a flexible carrier containing organic thin-film bilayer photovoltaic pixels; the pixels were arranged to provide the 2.5–4.5 V needed to operate the OEIP (Figure 8I).[155]

Magnetoelectric materials, which transform magnetic fields into electric fields through material properties instead of material configurations, have also been applied for wireless powering. Wickens et al. produced a magnetoelectric stimulator (ME) comprised of a magnetostrictive layer and piezoelectric layer, whereby the magnetic-field induced strain on the former exerts a force on the latter to generate a voltage. The ME could produce a variety of stimulation patterns in the 100–200 Hz therapeutic window. The authors also demonstrated that rice-sized ME films of different resonant frequencies could be individually addressed in a human phantom when stimulated by a magnetic field of the corresponding frequency.[156]

2.4. Substrates and Encapsulation

Choosing the appropriate substrate material and geometry for a given neural interface device requires the consideration of numerous factors, such as the device's intended duration of use, cost, manufacturability, depth of recording, target neuronal population size, and function (i.e., sensing, stimulation, or both). The specific substrate used in a probe governs probe properties, most essentially the biocompatibility of the device, but also stiffness, implantability, anchoring, performance of electrical signaling (including SNR, faradic and capacitive mechanisms, sensitivity, and selectivity), compatibility with nonelectronic signaling, and ease of implementation. Chronic implants (those with applications that require use for longer than 24 h) must not trigger an inflammatory response in tissue to maintain stability over long periods of time. Acute implants, on the other hand, need only resist acute inflammatory responses and prevent infection to maintain short-term stability. Probes that will be used on the surface of the skin generally must conform to the skin and may require an adhesive in order to anchor to the soft surface. Devices recording directly from the surface of groups of neurons, such as within cortical or spinal applications, must either conform to the neural surface or anchor into a rigid reference such as bone.

2.4.1. Hard Substrates

Early studies of neural interfaces employed hard substrates such as metal, glass and silicon. Hard substrates tend to have mechanical strength, resist ingress of liquids and vapors, and display particular manufacturability due to a large thermal budget (**Figure 9**A–E).[157]

Metals and Metal Oxides: Metal-based microelectrodes, smaller than ≈10 000 μm^2, can be used for more targeted stimulation and are generally used for ECoG and deep-brain applications. Commercially available microelectrodes, such as microwires (10–300 μm in diameter), are used for invasive neural interfaces and come in three main categories: single wire, tetrodes, and multi-wire arrays. Microwire tips can be flat or pointed, with pointed tips requiring smaller insertion forces.[158] Microwire arrays are customizable and can be obtained from manufacturers such as Blackrock Microsystems and PMT Corporation. Designed to record on the scale of individual neurons, these arrays must be carefully designed to prevent insulative layer delamination and avoid noise superimposition.[159,160] The small conduction areas in microelectrodes are much more susceptible to degradation from permanent faradic oxidation–reduction reactions—in particular when the stimulation waveform is not charge balanced. This is a common problem in Pt and PtIr electrodes.[161] However, these metal substrates are generally good candidates for surface modification with electrode-preserving capacitive charge injection as an alternative to faradic charge injection. Surface modification with coating can also be used to improve sensing. Titanium metal electrode substrates have good compatibility with TiN, which can be grown as a fractal (high surface area) thin film.

Commonly used metal substrates have favorable properties such as efficient transmission of neural signal frequencies and low inherent impedance. They are also compatible with surface modifications for tuning impedance in order to improve SNR.[55–57] Metal substrates are hard, but have low risk of brittle fracture, resist ingress of gases, vapor, and liquid, and can be detectable with MRI after implantation. However, there are limitations to the use of metal substrates. Metal substrates are often the electrode itself, therefore each metal electrode is limited to one signal along the conductor ("single channel") or requires expensive special fabrication. Due to the propensity toward permanent deformation of small metal probes, accidental bending has been reported to cause deviation from intended trajectory.[162] Furthermore, these electrodes are generally susceptible to deterioration during stimulation and require a charge balanced waveform or surface modification to enable capacitive charge injection. The inherent hardness of metal substrates makes these electrodes stiffer than surrounding tissue and has been widely observed to incite a fibrotic immune response, which also attenuates the neural signal.[102,163] The

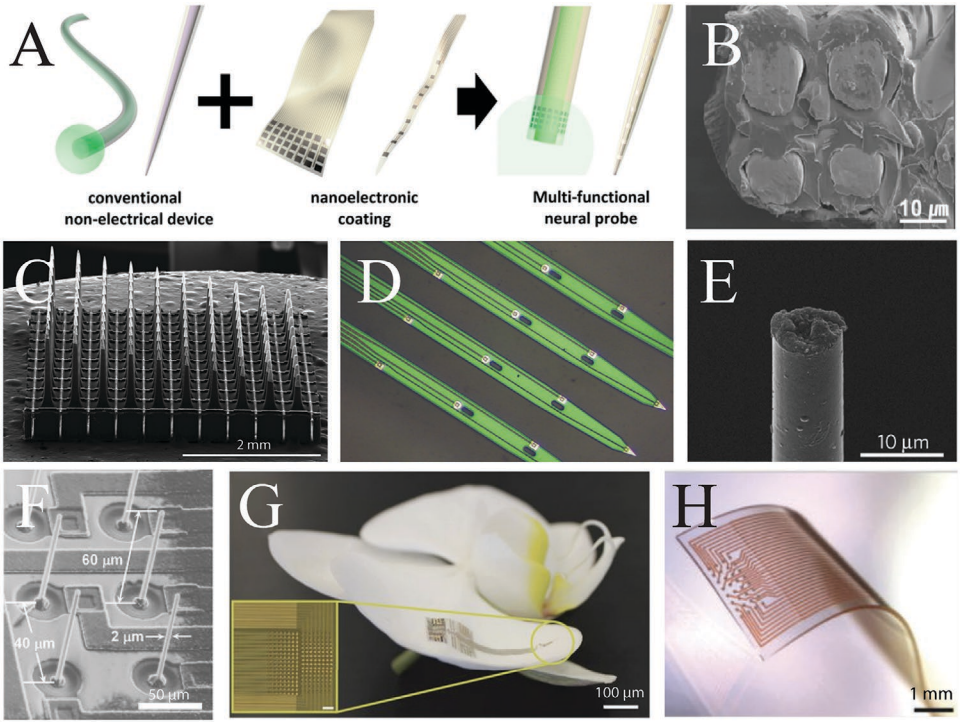

Figure 9. Examples of hard and soft substrates used in neural interfaces. A) Conventional optical fibers or glass pipettes become multifunctional neural probes upon application of nanoelectronic coatings (NECs). Reproduced with permission.[242] Copyright 2017, American Chemical Society. B) SEM of nichrome (NiCr) metal tetrode showing detail of metal substrate with polyimide insulation. Reproduced with permission.[243] Copyright 2018, The Korean Society for Brain and Neural Sciences. C) Utah Slant Electrode array with graduated penetration depths. Reproduced with permission.[244] Copyright 2014, Elsevier. D) Michigan probes, fabricated at the University of Michigan in 1994, built by bulk etching silicon substrates. E) Close-up of carbon substrate microthread with carbon core and poly(p-xylylene) coating. Reproduced with permission.[178] Copyright 2012, Springer Nature. F) Vapor-liquid-solid (VLS) silicon probes are mechanically flexible due to the growth direction and single-crystalline nature of silicon. Reproduced with permission.[245] Copyright 2010, Elsevier. G) Conformable parylene substrate with micropatterned gold electrodes and conductive traces. Reproduced with permission.[49] Copyright 2015, Springer Nature. H) Stretchable PDMS substrate with micropatterned conductive wires and electrodes. Reproduced with permission.[51] Copyright 2018, Wiley-VCH.

hardness of metal substrates can also result in cell death from implantation trauma. Metal substrates are generally fabricated with traditional fabrication techniques rather than microfabrication, making continued miniaturization expensive in both reducing electrode size and connecting electrodes to backend equipment.

Silicon, Glass, and Diamond: While metal substrates have been extensively studied, silicon and glass enable finer resolution in neural interfaces. Silicon micromachining is well defined for MEMS applications, and has been used to fabricate large, dense, parallel arrays for spinal cord, peripheral nerve fibers, ECoG, and intracortical recording.[57,164] Silicon substrates are not often used for noninvasive recordings, as they are best suited for recording microscale processes.[165] Silicon probes are generally used for recording, though monolithic circuitry built directly into silicon substrates has been used to develop two way neural interfaces.[166,167] Silicon substrates are prevalent in the semiconductor industry, making the integration of active or computational elements straightforward. Commercially available examples of silicon neural interface arrays are Utah arrays and Michigan probes. Utah arrays are usually limited to a few square millimeters in overall recording area and are made by bulk etching of a partially doped silicon wafer to form needle-like electrodes with fixed spacing, usually 40–300 µm in diameter. When inserted, the base of the Utah array floats over the area of insertion (such as the brain or spinal cord). Michigan probes are capable of greater depth insertion, but all the electrodes lie along the plane of the probe and are oriented on one side of the probe, which can result in "backside shielding" that affects signal processing of LFP.[53] Multiple electrodes are fabricated along the length of each comb in the array, and the implantation of these probes is largely similar to the insertion of a Utah array. The notable machinability and high-quality masking oxide material available for silicon processing also enables the formation of drug delivery cavities.[168]

Silicon probes provide considerable advantages over predecessor substrates due to silicon's inherent customizability. Silicon is arguably the most machinable substrate available for micromachining due to well-characterized processes and unique anisotropic properties. This machinability results in precise recording layouts and the ability to fabricate multiple channels along the length of a probe needle.[169] The increased number of channels allows for 3D recording at a density that was previously unattainable using metal probes. Further, the ubiquitous processes improve the consistency among probes in the array and lower production costs. Though silicon probes are widely used in neuroscience research applications, these probes must be used with caution. Silicon probes are brittle, and are prone to breaking due to handling during insertion.[162]

In addition, the useful size of the array is limited by the flatness of the silicon substrate in relation to the natural curvature of physiological tissue. Large arrays will not be able to penetrate these curved surfaces at a consistent depth, and therefore have limited usefulness. Silicon arrays are often used in research of large mammals and nonhuman primates, Utah arrays are FDA-approved for research in human subjects. Uncoated silicon will degrade over time with exposure to ionic fluid, and generally chronic probes require an insulative polymer coating.[170]

Since silicon probes may be susceptible to fouling, doped diamond probes have been also explored due to their biocompatibility, low capacitance, low fouling, and high charge density properties.[171,172] Some diamond probes are stiff like silicon, but if thinned sufficiently are somewhat flexible. However, the modulus of this material is still higher than that of adjacent tissue.[172] The ultimate issue to overcome with rigid probes is the modulus mismatch between the probe and native tissue at the implant site. This mismatch can lead to general drift in physical position, and a signal limiting glial encapsulation immune response which significantly impairs the signal integrity for chronic recording.[57,160,173,174]

2.4.2. Soft Substrates

Soft substrates are conducive to nearly all neural interface applications. For implanted probes, soft substrates have been developed with the goal of overcoming immune responses that attenuate signal, while retaining extremely small feature sizes (Figure 9F,G). Devices built on soft substrates are capable of recording high spatiotemporal resolution signals, from single neurons to micro-LFP. Commonly used soft substrates such as parylene-C, polyimide, and SU-8 have excellent compatibility with the microfabrication techniques that make silicon versatile, while having Young's moduli orders of magnitude lower.[157] The additional moldability of soft substrates can be leveraged to fabricate 3D structures with pockets to facilitate the growth of neurons into the probe or provide reservoirs for drug delivery.[175,176] Soft implants are usually inherently dielectric and are often used as the signal isolating insulative layer on the device. The modulus of soft implants must be carefully selected: if too soft, the implant can deteriorate, but if too hard, the implant can instigate an immune response. Soft substrates tend to have lower densities and are more compliant, making them comfortable for use as wearable external neural interfaces.

Flexible: With a long history as a final coating material for implanted medical devices, parylene-C is a Class VI implant grade material deposited by a highly conformable chemical vapor deposition process. Parylene resists immune response and moisture uptake, and therefore preserves recording signal strength over long periods of time.[177] The standard thickness for parylene substrates is very thin (<10 μm) but maintains integrity during handling. After fabrication, probes built on parylene substrates retain significant conformability, allowing them to conform on the surface of skin or neural tissue. Parylene can be coated over a hard substrate, such as a silicon wafer, and released after microfabrication of closely spaced thin film electrodes. This high-resolution fabrication process enables parylene devices to cover large areas, regardless of tissue curvature, at spike resolution.[49,178,179]

While polyimide has been shown to produce a lesser immune response than silicon does, it is not rated for long-term implantation. Polyimide substrates are fabricated with excellent thickness control by spin-coating precursor liquid onto the surface of a wafer, or by molding. Polyimide films can be etched slowly using photopatterning and solvent, but are more often patterned into their final shape using laser ablation, oxygen plasma or DRIE. Polyimide films require a final 400 °C baking cure step, which limits their compatibility with organic sensors that generally have a low thermal stress tolerance.[180] Once released, the polyimide substrate, usually between 10 and 50 μm thick, is still very flexible.[181] Because polyimide can be spin-coated to a range of desired thicknesses, it is often selected as a substrate for flexible neural interface devices.[123,182,183] Polyimide substrates are too flexible for penetration into the body without an additional "shuttle," a stiff support structure to facilitate implantation that is subsequently withdrawn.

A common soft lithography approach utilizes the photosensitive polymer SU-8 as mold material. SU-8 resist liquid comes in many spin-coating formulations to achieve thickness between 2 and 100 μm with excellent aspect ratio capability from manufacturers such as Microchem.[184,185] SU-8 substrates can be molded or spin-coated to fabricate flexible structures that are stiff enough to penetrate tissue, such as microneedles, while retaining control of small features.[186] These stiffer structures are an alternative to the structural shuttle needed for softer materials like polyimide and parylene.[187] However, SU-8 is not rated for long term implantation, and can be prone to breaking at the size needed to perform single neuron recording.

Stretchable: Flexible substrates are able to match the material properties of the surrounding tissue, but further material properties are necessary for interfacing with neurons in dynamic environments such as the spinal cord or peripheral nerves. Materials such as silicone derivatives can be molded and cured to form stretchable substrates (Figure 9H).[51,123] Minev et al. demonstrated the use of a flexible silicone probe for use in the spinal column that avoids the need for fixation, due to the inherent conformation of the silicone-based material.[142] Silicone can be customized to form a range of elastomers with different properties through different crosslinking mechanisms, conferring a high degree of versatility.[188] PDMS in particular has shown promise as a stretchable substrate.[51,189,190] Because stretchable substrates are able to re-form after significant deformation, there are opportunities for interfacing with dynamic surfaces.[191]

2.4.3. Environmentally Dependent Substrates

Soft materials enable significantly longer term implantation periods, but lack properties needed for ease of implantation and handling. Parylene and polyimide soft probes generally require a shuttle for deep brain access, and are at risk of folding or deforming during insertion, even when used with a support shuttle.[186] As seen with SU-8, there is a desire to forgo softness in order to fabricate a device hard enough to penetrate tissue during implantation.

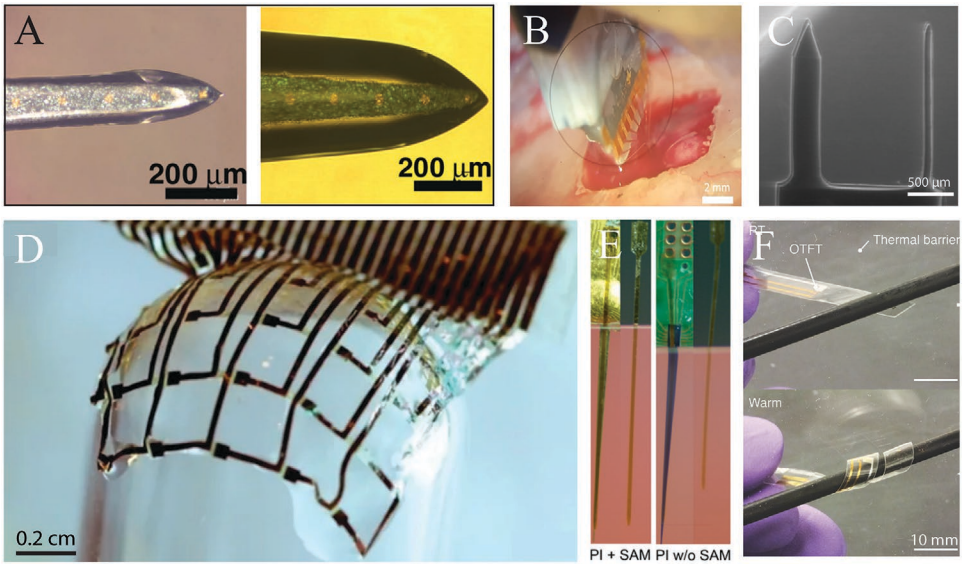

Figure 10. Environmentally dependent substrates have variable properties at different stages of use. A) Soft alginate hydrogel-coated silicon neural probe for improved early-stage integration with native tissue. Reproduced with permission.[192] Copyright 2009, Wiley-VCH. B) Thermally sensitive and water-softening neural probe with near-tissue modulus at room temperature. Reproduced with permission.[197] Copyright 2019, Springer Nature. C) Carboxymethylcellulose (CMC) dissolvable shuttle for insertion of compliant neural probes. Reproduced with permission.[246] Copyright 2014, Elsevier. D) Recording arrays made of ultrathin polyimide with silk support material. Reproduced with permission.[198] Copyright 2010, Springer Nature. E) Self-assembled monolayer (SAM)-coating of insertion shuttles improves flexible probe delamination. Reproduced with permission.[247] Copyright 2009, Elsevier. F) A planar OTFT deploys into a helix and wraps around a rod ($r = 2.25$ mm). Reproduced with permission.[248] Copyright 2014, Wiley-VCH.

Substrate materials that leverage the implant environment to dictate the stiffness of the material provide a solution to this problem. Examples of such materials are hydrogel-coated microneedles (**Figure 10**)[192,193–195] and thermoplastics, or thermally reactive copolymers that are implanted quickly and soften at biological temperatures.[196,197] In some cases, the structural support material for extremely thin probes can be used to improve manipulation during implantation, after which the support material dissolves into the water at the implant site. Kim et al. developed a device that utilized a silk support material, and was shown to conform tightly to the curvature of the brain after the support material dissolved.[198] Other dissolvable materials such as chitosan, maltose and PEG have been used as transient support structures that coat the soft device during implantation and subsequently dissolve. Recently, Rauhala et al. demonstrated the capacity to utilize chitosan for in vivo localization of neural interface devices and freestanding, stable, biocompatible films.[199] Use of these substrates opens the door to improved control over the implantation process.

In some cases, probes that require extensive surgery for implantation and healing will later require explant surgeries. The explant surgery puts the subject at risk of infection and necessitates the inconvenience of surgical healing a second time. The use of dissolvable metals such as Mg, Mo, Fe, and Zn—which are naturally found and essential to biological function in humans—was explored by Yin et al.[200] However, extensive studies on a completely dissolvable device have yet to be completed. Similarly, dissolvable biocompatible polymers such as polylactide, poly(ε-caprolactone), poly(polyol citrate) stretchable segmented poly-urethane, polyvinyl alcohol (PVA), poly(lactic-*co*-glycolic acid)(PLGA), and poly(polyol sebacate) may be used to control the lifetime of the device.[201,202]

2.4.4. Encapsulation

Early bare electrodes used for single neuron recording were often limited to use over hours or days, due to both size and biocompatibility of material. The stable life of electrodes was extended when materials such as stainless steel, tungsten, and platinum were miniaturized into microwires coated with electrical isolation polymers that enabled recording of durations up to nearly a year in primates.[57] However, electrodes exhibited wide variation and signal quality deteriorated over time, inspiring the first encapsulation for anti-inflammatory isolation.[203] Conducting material used for interconnects and internal components of implants must be electrically isolated outside of recording regions to ensure function. Some metal and silicon electrodes will degrade in ionic solutions, but are still fabricated from these materials for ease of manufacture and high controllability. Beyond basic stability and functionality, electrodes in biological systems must resist fouling and other immune responses to prevent signal variability and degradation over time.[55,57,162] Therefore, encapsulation techniques are used to retain the desirable substrate properties, often related to impedance and mechanical strength, while modifying the biological interface. Essential considerations are implant duration, substrate properties, and final form factor. Effective encapsulation prevents ingress of ions, fluids, and gases, acts as electrical isolation, and limits biological immune responses. In some applications, the encapsulation can also provide mechanical strength or promote integration with surrounding tissue.

Recording devices exposed to the biological environment must interact only as necessary to provide long term, stable recordings (**Figure 11**).

Techniques: Encapsulation techniques include coating, molding, and encapsulation within a housing, sometimes referred to as a "can." Each technique confers unique properties related to the size of the final product, conformability of the coating material and structural support. Coating techniques such as electrospinning, spraying, dipping, chemical vapor deposition (CVD) and physical vapor deposition (PVD) result in a roughly uniform increase in size. This approach is ideal for applications where the size of the implant must be minimized. Metal coatings are often deposited with PVD, while polymers are deposited via spraying, dipping, and CVD techniques.

Molding of electrodes usually involves polymers for their low process temperature, and is generally an irreversible process. Once set, the device is permanently encapsulated. Molding techniques allow for the embedded device to take on new shapes that can involve anchors or teeth for improved fixation. The material used to make the mold must be specially selected to release the encapsulation material after setting.

Devices with complex circuity that may need to be replaced, repaired, or inspected after use take advantage of housing approaches to encapsulation. Housing is made of stiff materials, to protect potentially fragile components within, and is welded to achieve a hermetic seal. Neural interfaces that are completely implanted, such as deep brain stimulation devices, have battery and circuit components encapsulated within a housing. This housing may also act as ground or reference for some sensing devices.

Finally, encapsulation may be part of the fabrication process itself, where a biocompatible polymer is both the substrate and encapsulation of the device. Examples of such an approach include devices with integrated antennas for communication, which may be fabricated monolithically.

Organic Materials: Epoxies were one of the first encapsulation mechanisms for chronically implanted devices (**Figure 12**A). However, these devices were prone to corrosion and degradation if the epoxy was not completely filled or any air gaps remained in the device. For more modern encapsulation techniques, the encapsulation takes place in a dehydrated, oxygen-free environment (often replaced with nitrogen) before hermetic sealing to limit corrosion of electronics.

Silicone derivatives are a commonly used encapsulation material in commercially available medical devices (Figure 12B,C). Silicone is biocompatible, biostable, straightforward to implement and is approved for use with implanted devices. Silicone in medical applications can be coated and cured at room temperature (common one-component room temperature vulcanizing (RTV) silicones use acetoxy or alkoxy reactions) or dip coated thinly (about 100 µm) and vulcanized with heat to the final state. Thixotropic non-slump silicone is viscous and can be used to selectively coat the device surface. Self-leveling silicone is thin and can be used for potting or molding. However, silicone coatings are not perfectly conformal, tend to be somewhat thick, and may shear under pressure if not vulcanized.

Polyurethane is more expensive than other coating materials and is not rated for permanent implantation as it tends to degrade over several years. However, polyurethane is an extremely versatile polymer in which the ratios of soft backbone and hard diisocyanate components can be adjusted to create elastomers or hard plastics. It can be fabricated using a wide range of techniques

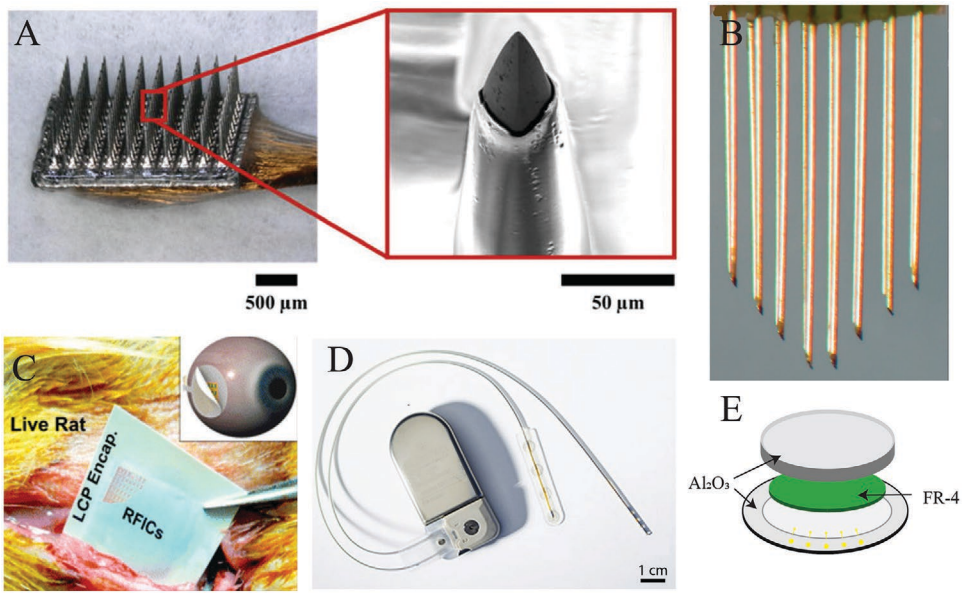

Figure 11. Encapsulation techniques for neural-interface devices. A) Parylene-C coated silicon shafts of Utah array. Reproduced with permission.[249] Copyright 2019, Springer Nature. B) Polyimide-insulated tungsten microwires. Reproduced with permission.[257] Copyright 2018, T. D. Y Kozai. C) Low-water-absorption liquid-crystal polymer (LCP) encapsulated retinal electrode. Reproduced with permission.[209] Copyright 2013, American Chemical Society. D) Metal housing used by NeuroPace, such as FDA approved biocompatible titanium. Such housings are often welded closed for a hermetic seal and further coated with parylene-C as a precautionary measure. Adapted with permission.[258] Copyright 2015, Elsevier. E) Ceramic encapsulation of flame retardant-4 (FR-4)-based printed circuit board (PCB). Feedthroughs are metal tracks on ceramic substrate.

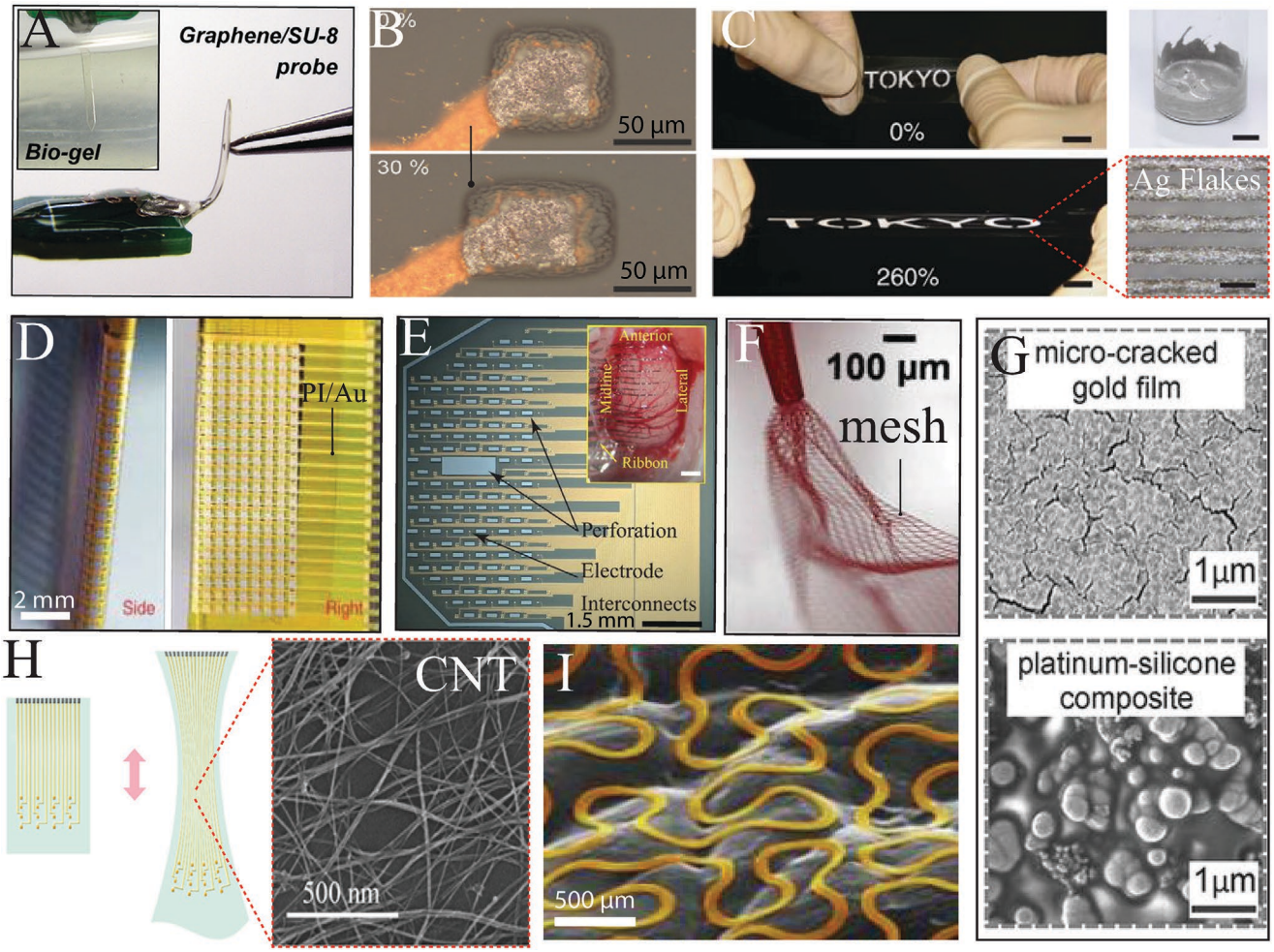

Figure 12. Flexible and stretchable interconnect. A) Flexible SU-8 probe deposited on graphene and insulated with PDMS, where graphene acts as single-signal conductor. SU-8 provides sufficient stiffness to penetrate tissue Reproduced with permission.[250] Copyright 2013, Elsevier. B) Au–TiO nanowires on stretchable PDMS substrate, shown before and after 30% extension. Reproduced with permission.[51] Copyright 2018, Wiley-VCH. C) Use of silver flakes as a conductive filler in elastomeric fluorine copolymer embedded to make conductive ink. Ink is printed onto into stretchable PDMS substrate, and retains conductivity of more than 100 S cm^{-1} up to 260% stretching. Reproduced with permission.[223] Copyright 2015, Springer Nature. D) Flexible polyimide device with gold conductor traces interconnecting flexible silicon nanomembrane transistors. Cable is robust enough to be folded in half and retain conductivity. Reproduced with permission.[79] Copyright 2011, Springer Nature. E) PEDOT:PSS electrodes on highly conformable ultrathin optically clear parylene substrate improves visualization of electrode placement. Highly conformable properties fix probe to location while perforations tolerated by parylene substrate allow CSF flow. Reproduced with permission.[251] Copyright 2017, AAAS. F) FET nanoprobes integrated into flexible SU-8 substrate result in injectable neural probes. Reproduced with permission.[219] Copyright 2018, Elsevier. G) Stretchable thin film cracked gold interconnects (top) and Pt–silicone stretchable composite as electrode material (bottom). Reproduced with permission.[142] Copyright 2015, AAAS. H) Stretchable PDMS ribbon with transparent carbon nanotube conductors transmitting electrode signal to recording area with electrochemical impedance below 0.4 MΩ in 7.4 pH saline for sensing compatible with optogenetic stimulation. Reproduced with permission.[222] Copyright 2018, American Chemical Society. I) Stretchable gold serpentine shapes over a skin replica material, with SEM image artificially colored to highlight conformal contact over topography. Reproduced with permission.[225] Copyright 2014, Springer Nature.

including extrusion, dipping, and molding. Polyurethane has unique toughness that can be used to form strong, thin flexible cables.[204] For medical applications, polyurethanes with aromatic diisocyanates are preferred for favorable chemical resistance. The soft backbone component traditionally used in cardiac applications makes the polymer hydrophobic, but can be replaced with another polymer such as PEG to create a biocompatible nonfouling hydrogel.[205] Polyurethane formulations have also been shown to be compatible with antimicrobial additives such as silver.[206] For neural applications, use of polyurethanes is generally found on metal probes rather than silicon.

Polyimide is a biocompatible coating with excellent electrical insulation properties that can be coated as thin as 7 µm (Figure 12D). Polyimide is a common coating material for microwire electrodes, coated everywhere and then ablated in regions to be exposed. However, over time polyimide coatings show wear when exposed to aqueous environments and many formulations are not suitable for chronic implantation.[207,208] Companies such as Tucker-Davis Technologies fabricate probes with polyimide-insulated tungsten arrays.

Liquid crystal polymer (LCP) is a promising material for encapsulation with limited commercial adoption. LCP is

a thermoplastic that is typically molded into a final form, such as films for coating or extruded as a coating for wires. Among LCP's favorable properties are extreme resistance to water ingress, biostability, and reliable dielectric properties. The limited adoption of LCP is often due to poor adhesion of LCP to other materials and limited encapsulation techniques, making LCP best for applications where preformed LCP can be used.[209–213]

Finally, parylene-C is used in applications where a truly conformal coating is desired (Figure 12E). Parylene is deposited by transferring a dimeric gas directly onto the part to be coated. As parylene is deposited onto the device, thin layers are formed with low pinhole occurrence. This extremely thin layer shows excellent biocompatibility is can be used as a secondary coating after other encapsulation techniques are used.[214] Often even hermetically sealed devices have an additional parylene coating for increased reliability.

Teflon (PTFE) is a polymer that can be deposited with CVD, like parylene. Teflon is extremely nonreactive and can be used as a lubricous or nonfouling surface. Teflon has a hydrophilic surface, and can be used to generally prevent sticking between parts.

Inorganic Materials: Metals and metal oxides have been used to modify substrates in a variety of ways. From small modifications that improve the conductive tissue-device interface to sturdy encapsulation housings, certain metals enhance the device-tissue interface.[160] Metals for housings include titanium, nickel-titanium (nitinol), stainless steel, and cobalt-chrome, which have good strength and wear resistance. Gold, tantalum, and platinum are stable in the body but due to their soft nature are not usually structural elements in a device. However, tantalum can be incorporated into the encapsulation to provide detectability after implantation.

The gold standard for commercial neural devices with circuitry is a titanium can coated with parylene for additional protection. Titanium has a history of exceptional biostability and biocompatibility for chronic implantation. These shells are sealed for hermeticity to prevent moisture from affecting the circuitry inside, and often are filled with inert gas, such as nitrogen, and a desiccant for additional protection from corrosion. Brands like NeuroPace and NeuroVista build closed loop seizure detection systems that are completely implanted in the body. Both devices utilize a titanium can, embedded into the skull or chest tissue, to protect electronics from corrosion.

Glass encapsulation has not been demonstrated with modern neural probes, but has been shown to be possible in other long-term implanted medical devices. CardioMEMS, a blood pressure monitor placed within the pulmonary artery, is encased in glass using anodic bonding of two extremely flat glass surfaces.

Ceramic encapsulation is commercially available through companies such as CorTec, which are able to fabricate many electrode access holes due to superior machinability. Ceramics are ideal for applications where the encapsulation must be electromagnetically transparent, such as for devices that rely on communication via radiofrequency or infrared, or are powered inductively. Ceramic encapsulation has also been found to outlast standard titanium housing packaging in moisture resistance.

2.5. Interconnects and Connector Materials

Neural interfaces collect signals on the order of tens to hundreds of microvolts, which must then be amplified and filtered. Interconnects are essential parts of neural interface systems, connecting the signal collected at the electrode to backend signal acquisition, such as preamplifiers or acquisition PCBs. Signals that must traverse the interconnects can be either analog or digital, depending on the probe digitization scheme. In order to maintain the integrity of the electrode location, interconnects should be able to handle the changing relative positions of the electrodes and backend of neural interfaces. In early silicon neural interface devices, wires coated with nonreactive PTFE extended from the electrode to the backend.[162] However, the stiffness of connector wires limited connection of devices to backend electronics that were mounted to a fixed location such as the skull. The inherent mechanical forces and torque on the wire would dislodge probes recording from locations such as the spinal cord and peripheral nervous system, spurring the need for solutions to decouple these mechanical forces.[162] Furthermore, the interconnect scheme is often a bottleneck limiting the miniaturization of devices. As the number of recording sites that can be simultaneously recorded increases, the connector must be able to scale alongside the technology to transmit data to backend processing.

2.5.1. Ribbon

Ribbon cables relieve forces between electrode and backend by bending and warping to accommodate movement (**Figure 13**). Ribbon cables can be flexible or stretchable, usually with a dielectric insulating substrate containing a conductor able to retain conductive properties when manipulated. The ribbon is responsible for sending electrical or optical signals over the distance between the recording electrode and backend processing.

Flexible: Flexible ribbon cables can be built on substrates such as polyimide, parylene-C and SU-8. Ribbon cables must be robust enough to maintain integrity when bent, folded, and connected to backend equipment. Polyimide flexible interconnect cables are often integrated directly onto electrode probes, maintaining flexibility over the length of extension to backend, which can be multiple centimeters in length. The high-temperature resistance of polyimide, also known as Kapton, makes it compatible with solder-bond pads.[79,181,183,215,216] Polyimide cables also have the stiffness necessary to be used with zero insertion force (ZIF) connectors.[217] The higher thickness of polyimide provides sufficient insulation and has low likelihood of forming pinholes, which may otherwise compromise the integrity of the signal transmission. However, because polyimide is not rated for long term implantation due to high moisture uptake (≈4 wt%),[177] benzocyclobutane has been demonstrated as an alternative by Lee at al. In this device, microfluidic channels were incorporated into the ribbon as well, making the ribbon effective for both electrical communication and fluid transfer. For applications where the environment is more dynamic, parylene-C ribbon cables are flexible and thinner than polyimide.[92,218] In addition, parylene is rated for long-term implantation, conferring another advantage

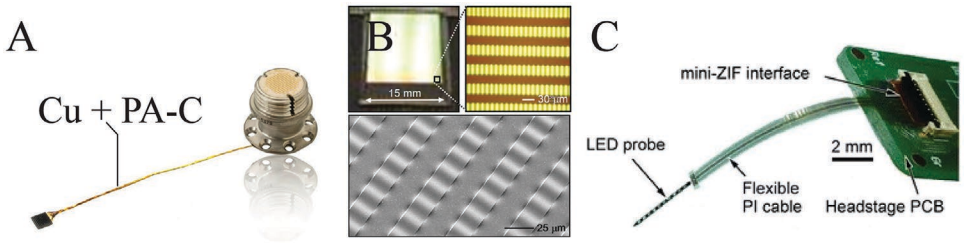

Figure 13. Examples of ribbons used to carry electrode information. A) Bundled Au wire cable with parylene insulation that does not decouple mechanical forces from connector, Reproduced with permission.[259] Copyright 2007, Elsevier. B) Array of wavy, single-crystal silicon ribbons on PDMS (top left); individual ribbons are visible (top right, bottom). Reproduced with permission.[252] Copyright 2006, AAAS. C) Fully integrated flexible polyimide ribbon cable. Reproduced with permission.[253] Copyright 2017, Springer Nature.

over polyimide in some situations. Using parylene, Hong et al. developed a large-scale mesh of electrodes.[219] This parylene interconnect scheme was robust enough to be forced into a needle, injected into the brain, and allowed to unfurl. The interconnect allowed signal from many recording sites to be transferred to backend processing while matching the mechanical properties of the tissue through which it traversed. For applications where optically transparent properties are necessary for the interface, the use of ITO was investigated, but was found to be unable to flex due to its brittle nature and limited by high temperature processing. Instead, the use of graphene on SU-8 and PDMS creates a conductive, optically transparent ribbon that is also capable of flexing.[220]

Stretchable: Flexible substrates are excellent for applications where mechanical properties of tissue must be matched, but these substrates generally cannot handle elongation through stretching. Stretchable ribbon cables open the door to neural interfaces in highly dynamic environments such as the spinal cord and peripheral nervous system. Standard thin film deposition, if deposited incorrectly, will delaminate and break when the stretchable substrate material is deformed.[79] However, it has been shown that some gold patterned films deposited on prestretched substrates are able to form forgiving microcracks that maintain conductivity when stretched (Figure 12G).[176,190] The use of nanostructures such as gold and silver nanowires can preserve conductivity of 5285 S cm^{-1} (original conductivity 8130 S cm^{-1}, sheet resistance 0.25 Ω $\square^{-1}$) even after repeated stretching to 1.5 times the original length.[189] However, the resistance of carbon nanotubes (CNTs), gold nanowires (AuNW), silver nanowires (AgNW) and silver nanoparticles (AgNPs) will vary with respect to elongation, warping the recorded signal (Figure 12H,I).[51,189,221–223] Devices utilizing these technologies require characterization of impedance changes for use. Beyond stretchable materials, serpentine ribbon cables can rely on the low impedance properties of conventional metals using a serpentine shape, functioning like a spring to decouple movement. These serpentine shapes can be fabricated at many length scales, including atomic scales as shown by Tang et al. with CNT on PDMS.[224] Combinations of serpentine patterns in complementary positions elicit stretch compatibility with additional degrees of freedom.[225,226] For applications where it is essential for the ribbon to maintain conductivity but also optical transparency during stretching, it has been shown that CNT on PDMS can be used to monitor neural circuits with both electrical and optical approaches.[222]

2.5.2. Connectors

It is necessary to create connectors that bridge the differences in conductor schemes, substrate properties, physical location, and signal postprocessing technology. Connectors represent the scheme used to transfer neural information from the interconnects to the backend recording system, and dictate the scalability, manufacturability, and integrity of the data transfer over time. Technologic advancements that produced microarrays on the 100 μm scale were able to achieve high recording site density but involved cumbersome wire bonding, bundling, and probe guiding techniques (**Figure 14**A–D). Hard substrates such as silicon and other MEMS probes are compatible with fusion, eutectic, anodic, and wire bonding systems.[227–229] An alternative to wire bonding, which requires large equipment, is solder ball bonding. This process is heat-activated and allows a connector with well controlled dimensions to be reflowed and connect to the probe electrode.[228] However, softer substrates have limited compatibility with wire bonding equipment, especially as the contact pad sizes have decreased. Anisotropic conductive films and paste have been used to selectively connect flexible substrates with greater ease.[198] Bumps fabricated into the films make it possible to reliably connect films, but thermocompressive equipment is necessary to control the process. With proper pressure and temperature optimization, these films can be extremely reliable connectors for soft electrodes.[230] Recently, Jastrzebska-Perfect et al. introduced an organic mixed-conducting particulate composite material (MCP) that enables facile and effective electronic bonding between soft and rigid electronics (Figure 14E).[231] Ultimately, monolithic connectors in which the flexible ribbon is connected to the device during fabrication, in particular using semiconductor processes, provide the highest manufacturability. This is an extremely scalable process, and can be used to connect hundreds of electrodes in tandem.[125,166]

3. Conclusion

Neuroelectronics are critical for the diagnosis and treatment of several neuropsychiatric conditions, and are hypothesized to have many more applications. A wide variety of materials and approaches have been utilized to create innovative neuroelectronic device components, from the tissue interface and acquisition electronics to interconnects and encapsulation.

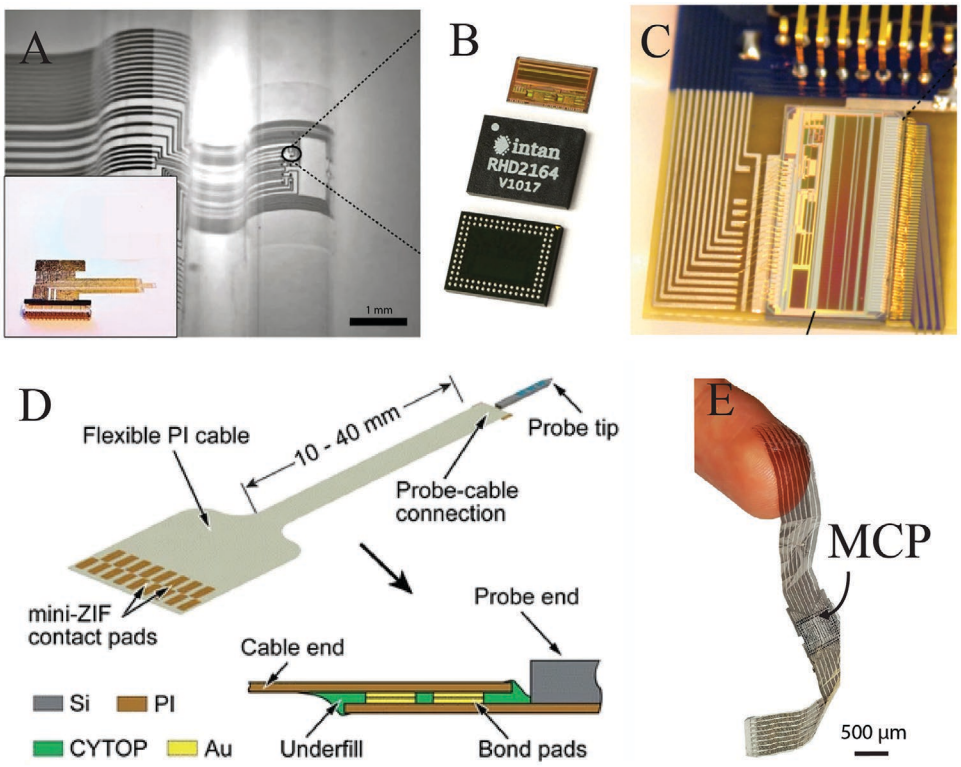

Figure 14. Examples of connectors and used in neuroelectronics. A) Conformable probe with zero insertion force (ZIF) connector. Adapted with permission.[92] Copyright 2013, Springer Nature. B) Ball bonding chips (BGA) from Intan used to amplify recorded neural signals can be placed over a contact pad array and reflowed in an oven to robustly connect the chip. Adapted with permission.[260] Copyright 2020, Intan Technologies. C) Device with wire-bonded connectors on resin PCB connecting ZIF housing to backend circuitry. Reproduced with permission.[254] Copyright 2011, PLOS. D) Polyimide (PI) probe flip-chip bonded to PI cable. Probe-cable interface is underfilled with fluoropolymer CYTOP to increase mechanical stability. Reproduced with permission.[253] Copyright 2017, Springer Nature. E) Microscopy images of two conformable arrays bonded together by MCP; arrow indicates the bonding area. Reproduced with permission.[231] Copyright 2020, AAAS.

Although traditional materials have a strong track record of stability and safety within a narrow range of use, many of their properties are suboptimal for chronic implantation in body tissue. Material advances harnessed to form all the components required for fully integrated neuroelectronic devices hold promise for improving the long-term efficacy and biocompatibility of these devices within physiological environments. Consequently, these advances would allow simpler and safer testing in animal models and ultimately human subjects, increasing the potential for clinical translation that could improve the quality of life for patients with neuropsychiatric diseases.

Acknowledgements

P.J.-P. and S.C. contributed equally to this work. This work was supported by Columbia University, School of Engineering and Applied Science, as well as Columbia University Medical Center, Department of Neurology and Institute for Genomic Medicine. G.D.S. is supported through the Human Frontiers Postdoctoral Fellowship Program. This work was supported by the NIH grant (1U01NS108923-01), NSF CAREER (1944415), CURE Taking Flight Award, Columbia School of Engineering.

Conflict of Interest

The authors declare no conflict of interest.

Keywords

bioelectronics, clinical translational, neural interface devices

Received: November 4, 2019
Revised: February 6, 2020
Published online: June 8, 2020

[1] C. Gold, D. A. Henze, C. Koch, G. Buzsáki, *J. Neurophysiol.* **2006**, *95*, 3113.
[2] G. Buzsáki, C. A. Anastassiou, C. Koch, *Nat. Rev. Neurosci.* **2012**, *13*, 407.
[3] N. Kuhnke, J. Schwind, M. Dümpelmann, M. Mader, A. Schulze-Bonhage, J. Jacobs, *Brain Topogr.* **2018**, *31*, 1059.
[4] J. X. Tao, A. Ray, S. Hawes-Ebersole, J. S. Ebersole, *Epilepsia* **2005**, *46*, 669.
[5] M. Balish, R. Muratore, *Adv. Neurol.* **1990**, *54*, 79.
[6] M. F. Selvitelli, L. M. Walker, D. L. Schomer, B. S. Chang, *J. Clin. Neurophysiol.* **2010**, *27*, 87.
[7] N. Maromi, J. M. Lee, V. L. Shanker, M. R. Sperling, *Epilepsia* **1999**, *40*, 157.
[8] D. Friedman, J. Claassen, L. J. Hirsch, *Anesth. Analg.* **2009**, *109*, 506.
[9] J. Cappell, C. Schevon, R. G. Emerson, *Curr. Neurol. Neurosci. Rep.* **2006**, *6*, 327.
[10] T. R. Henry, D. A. Ross, L. A. Schuh, I. Drury, *J. Clin. Neurophysiol.* **1999**, *16*, 426.

[11] I. S. Fernández, T. Loddenkemper, *J. Clin. Neurophysiol.* **2013**, *30*, 554.
[12] P. Dahal, N. Ghani, A. Flinker, P. Dugan, D. Friedman, W. Doyle, O. Devinsky, D. Khodagholy, J. N. Gelinas, *Brain* **2019**, *142*, 3502.
[13] A. Thomschewski, A. S. Hincapié, B. Frauscher, *Front. Neurol.* **2019**, *10*.
[14] E. M. Merricks, E. H. Smith, G. M. McKhann, R. R. Goodman, L. M. Bateman, R. G. Emerson, C. A. Schevon, A. J. Trevelyan, *Brain* **2015**, *138*, 2891.
[15] E. Hedegärd, J. Bjellvi, A. Edelvik, B. Rydenhag, R. Flink, K. Malmgren, *J. Neurol. Neurosurg. Psychiatry* **2014**, *85*, 716.
[16] J. R. Daube, D. I. Rubin, *Muscle Nerve* **2009**, *39*, 244.
[17] B. Katirji, *Neurol. Clin.* **2002**, *20*, 291.
[18] J. Kimura, *Muscle Nerve* **1997**, *20*, 777.
[19] J. W. Albers, P. D. Donofrio, T. K. McGonagle, *Muscle Nerve* **1985**, *8*, 528.
[20] M. Pollay, *Neurosurgery* **1993**, *32*, 325.
[21] P. Ballabh, A. Braun, M. Nedergaard, *Neurobiol. Dis.* **2004**, *16*, 1.
[22] L. H. Jimison, S. A. Tria, D. Khodagholy, M. Gurfinkel, E. Lanzarini, A. Hama, G. G. Malliaras, R. M. Owens, *Adv. Mater.* **2012**, *24*, 5919.
[23] K. Wesemann, R. J. Coffey, M. S. Wallace, Y. Tan, S. Broste, A. Buvanendran, *Reg. Anesth. Pain Med.* **2014**, *39*, 341.
[24] W. Ilias, B. le Polain, E. Buchser, L. Demartini, J. Neuhold, W. Schleinzer, S. Eldabe, J. Maeyaert, E. Reig, G. Fortini, A. Ver Donck, H. Glawe, J. R. Gonzaléz-Escalada, V. Heidecke, A. Costantini, T. Riegel, R. Becker, A. Seeliger, *Pain Pract.* **2008**, *8*, 164.
[25] O. Sagher, D. L. Huang, *Neurosurg. Focus* **2006**, *21*, E2.
[26] C. A. Odonkor, S. Orman, V. Orhurhu, M. E. Stone, S. Ahmed, *Pain Med.* **2019**, *20*, 2479.
[27] I. Orosz, D. McCormick, N. Zamponi, S. Varadkar, M. Feucht, D. Parain, R. Griens, L. Vallée, P. Boon, C. Rittey, A. K. Jayewardene, M. Bunker, A. Arzimanoglou, L. Lagae, *Epilepsia* **2014**, *55*, 1576.
[28] J. E. Stevens-Lapsley, J. E. Balter, P. Wolfe, D. G. Eckhoff, W. M. Kohrt, *Phys. Ther.* **2012**, *92*, 210.
[29] M. A. Nitsche, W. Paulus, *J. Physiol.* **2000**, *527*, 633.
[30] N. E. O'Connell, B. M. Wand, L. Marston, S. Spencer, L. H. Desouza, *Cochrane Database Syst. Rev.* **2014**, *2014*.
[31] D. M. Blumberger, F. Vila-Rodriguez, K. E. Thorpe, K. Feffer, Y. Noda, P. Giacobbe, Y. Knyahnytska, S. H. Kennedy, R. W. Lam, Z. J. Daskalakis, J. Downar, *Lancet* **2018**, *391*, 1683.
[32] A. P. Trevizol, P. Shiozawa, I. A. Cook, I. A. Sato, C. B. Kaku, F. B. Guimarães, P. Sachdev, S. Sarkhel, Q. Cordeiro, *J. ECT* **2016**, *32*, 262.
[33] T. A. Dembek, P. Reker, V. Visser-Vandewalle, J. Wirths, H. Treuer, M. Klehr, J. Roediger, H. S. Dafsari, M. T. Barbe, L. Timmermann, *Mov. Disord.* **2017**, *32*, 1380.
[34] T. A. Zesiewicz, R. J. Elble, E. D. Louis, G. S. Gronseth, W. G. Ondo, R. B. Dewey, M. S. Okun, K. L. Sullivan, W. J. Weiner, *Neurology* **2011**, *77*, 1752.
[35] E. Moro, C. LeReun, J. K. Krauss, A. Albanese, J. P. Lin, S. Walleser Autiero, T. C. Brionne, M. Vidailhet, *Eur. J. Neurol.* **2017**, *24*, 552.
[36] L. Perestelo-Pérez, A. Rivero-Santana, J. Pérez-Ramos, P. Serrano-Pérez, J. Panetta, P. Hilarion, *J. Neurol.* **2014**, *261*, 2051.
[37] E. Krook-Magnuson, J. N. Gelinas, I. Soltesz, G. Buzsáki, *JAMA Neurol.* **2015**, *72*, 823.
[38] D. M. Schultz, L. Webster, P. Kosek, U. Dar, Y. Tan, M. Sun, *Pain Physician* **2012**, *15*, 1.
[39] P. Hamilton, I. Soryal, P. Dhahri, W. Wimalachandra, A. Leat, D. Hughes, N. Toghill, J. Hodson, V. Sawlani, T. Hayton, S. Samarasekera, M. Bagary, D. McCorry, R. Chelvarajah, *Seizure* **2018**, *58*, 120.
[40] C. Anidi, J. J. O'Day, R. W. Anderson, M. F. Afzal, J. Syrkin-Nikolau, A. Velisar, H. M. Bronte-Stewart, *Neurobiol. Dis.* **2018**, *120*, 107.
[41] B. C. Jobst, R. Kapur, G. L. Barkley, C. W. Bazil, M. J. Berg, G. K. Bergey, J. G. Boggs, S. S. Cash, A. J. Cole, M. S. Duchowny, R. B. Duckrow, J. C. Edwards, S. Eisenschenk, A. J. Fessler, N. B. Fountain, E. B. Geller, A. M. Goldman, R. R. Goodman, R. E. Gross, R. P. Gwinn, C. Heck, A. A. Herekar, L. J. Hirsch, D. King-Stephens, D. R. Labar, W. R. Marsh, K. J. Meador, I. Miller, E. M. Mizrahi, A. M. Murro, D. R. Nair, K. H. Noe, P. W. Olejniczak, Y. D. Park, P. Rutecki, V. Salanova, R. D. Sheth, C. Skidmore, M. C. Smith, D. C. Spencer, S. Srinivasan, W. Tatum, P. Van Ness, D. G. Vossler, R. E. Wharen, G. A. Worrell, D. Yoshor, R. S. Zimmerman, T. L. Skarpaas, M. J. Morrell, *Epilepsia* **2017**, *58*, 1005.
[42] E. B. Geller, T. L. Skarpaas, R. E. Gross, R. R. Goodman, G. L. Barkley, C. W. Bazil, M. J. Berg, G. K. Bergey, S. S. Cash, A. J. Cole, R. B. Duckrow, J. C. Edwards, S. Eisenschenk, J. Fessler, N. B. Fountain, A. M. Goldman, R. P. Gwinn, C. Heck, A. Herekar, L. J. Hirsch, B. C. Jobst, D. King-Stephens, D. R. Labar, J. W. Leiphart, W. R. Marsh, K. J. Meador, E. M. Mizrahi, A. M. Murro, D. R. Nair, K. H. Noe, Y. D. Park, P. A. Rutecki, V. Salanova, R. D. Sheth, D. C. Shields, C. Skidmore, M. C. Smith, D. C. Spencer, S. Srinivasan, W. Tatum, P. C. Van Ness, D. G. Vossler, R. E. Wharen, G. A. Worrell, D. Yoshor, R. S. Zimmerman, K. Cicora, F. T. Sun, M. J. Morrell, *Epilepsia* **2017**, *58*, 994.
[43] M. B. Lee, D. R. Kramer, T. Peng, M. F. Barbaro, C. Y. Liu, S. Kellis, B. Lee, *J. Clin. Neurosci.* **2019**, *68*, 13.
[44] A. B. Ajiboye, F. R. Willett, D. R. Young, W. D. Memberg, B. A. Murphy, J. P. Miller, B. L. Walter, J. A. Sweet, H. A. Hoyen, M. W. Keith, P. H. Peckham, J. D. Simeral, J. P. Donoghue, L. R. Hochberg, R. F. Kirsch, *Lancet* **2017**, *389*, 1821.
[45] L. Resnik, F. Acluche, S. Lieberman Klinger, M. Borgia, *Prosthet. Orthot. Int.* **2018**, *42*, 534.
[46] A. L. Benabid, T. Costecalde, A. Eliseyev, G. Charvet, A. Verney, S. Karakas, M. Foerster, A. Lambert, B. Morinière, N. Abroug, M.-C. Schaeffer, A. Moly, F. Sauter-Starace, D. Ratel, C. Moro, N. Torres-Martinez, L. Langar, M. Oddoux, M. Polosan, S. Pezzani, V. Auboiroux, T. Aksenova, C. Mestais, S. Chabardes, *Lancet Neurol.* **2019**, *4422*, 1.
[47] C. M. Loftus, M. Hoffmann, W. Heetderks, X. Zheng, C. Peña, *Front. Neurol.* **2018**, *9*, 320.
[48] Regulatory Overview for Neurological Devices, FDA.
[49] D. Khodagholy, J. N. Gelinas, T. Thesen, W. Doyle, O. Devinsky, G. G. Malliaras, G. Buzsáki, *Nat. Neurosci.* **2015**, *18*, 310.
[50] A. J. Bard, L. R. Faulkner, J. Leddy, C. G. Zoski, *Electrochemical Methods: Fundamentals and Applications*, Vol. *2*, Wiley, New York **1980**.
[51] K. Tybrandt, D. Khodagholy, B. Dielacher, F. Stauffer, A. F. Renz, G. Buzsáki, J. Vörös, *Adv. Mater.* **2018**, *30*, 1706520.
[52] J. J. Jun, N. A. Steinmetz, J. H. Siegle, D. J. Denman, M. Bauza, B. Barbarits, A. K. Lee, C. A. Anastassiou, A. Andrei, Ç. Aydın, M. Barbic, T. J. Blanche, V. Bonin, J. Couto, B. Dutta, S. L. Gratiy, D. A. Gutnisky, M. Häusser, B. Karsh, P. Ledochowitsch, C. M. Lopez, C. Mitelut, S. Musa, M. Okun, M. Pachitariu, J. Putzeys, P. D. Rich, C. Rossant, W. Sun, K. Svoboda, M. Carandini, K. D. Harris, C. Koch, J. O'Keefe, T. D. Harris, *Nature* **2017**, *551*, 232.
[53] G. Buzsáki, E. Stark, A. Berényi, D. Khodagholy, D. R. Kipke, E. Yoon, K. D. Wise, *Neuron* **2015**, *86*, 92.
[54] E. S. Lein, M. J. Hawrylycz, N. Ao, M. Ayres, A. Bensinger, A. Bernard, A. F. Boe, M. S. Boguski, K. S. Brockway, E. J. Byrnes, L. Chen, T. M. Chen, M. C. Chin, J. Chong, B. E. Crook, A. Czaplinska, C. N. Dang, S. Datta, N. R. Dee, A. L. Desaki, T. Desta, E. Diep, T. A. Dolbeare, M. J. Donelan, H. W. Dong, J. G. Dougherty, B. J. Duncan, A. J. Ebbert, G. Eichele, L. K. Estin, et al., *Nature* **2007**, *445*, 168.

[55] R. Chen, A. Canales, P. Anikeeva, *Nat. Rev. Mater.* **2017**, *2*, 16093.
[56] S. M. Wellman, J. R. Eles, K. A. Ludwig, J. P. Seymour, N. J. Michelson, W. E. McFadden, A. L. Vazquez, T. D. Y. Kozai, *Adv. Funct. Mater.* **2018**, *28*, 1701269.
[57] M. Jorfi, J. L. Skousen, C. Weder, J. R. Capadona, *J. Neural Eng.* **2015**, *12*, 011001.
[58] P. R. Troyk, S. F. Cogan, in *Neural Engineering* (Ed: B. He), Kluwer Academic Publishers: New York **2005**, pp. 1–48.
[59] N. V. Apollo, M. I. Maturana, W. Tong, D. A. X. Nayagam, M. N. Shivdasani, J. Foroughi, G. G. Wallace, S. Prawer, M. R. Ibbotson, D. J. Garrett, *Adv. Funct. Mater.* **2015**, *25*, 3551.
[60] L. A. Geddes, R. Roeder, *Biomed. Eng.* **2003**, *31*, 879.
[61] R. Green, M. R. Abidian, *Adv. Mater.* **2015**, *27*, 7620.
[62] M. R. Abidian, K. A. Ludwig, T. C. Marzullo, D. C. Martin, D. R. Kipke, *Adv. Mater.* **2009**, *21*, 3764.
[63] X. Cui, D. C. Martin, *Sens. Actuators, B.* **2003**, *89*, 92.
[64] D.-H. Kim, J. A. Wiler, D. J. Anderson,D. R. Kipke,D. C. Martin, *Acta Biomater.* **2010**, *6*, 57.
[65] D. A. Koutsouras, P. Gkoupidenis, C. Stolz, V. Subramanian, G. G. Malliaras, D. C. Martin, *ChemElectroChem* **2017**, *4*, 2321.
[66] K. A. Ludwig, J. D. Uram, J. Yang, D. C. Martin, D. R. Kipke, *J. Neural Eng.* **2006**, *3*, 59.
[67] P. G. Taylor, J. K. Lee, A. A. Zakhidov, M. Chatzichristidi, H. H. Fong, J. A. DeFranco, G. G. Malliaras, C. K. Ober, *Adv. Mater.* **2009**, *21*, 2314.
[68] A. A. Zakhidov, J. K. Lee, J. A. Defranco, H. H. Fong, P. G. Taylor, M. Chatzichristidi, C. K. Ober, G. G. Malliaras, *Chem. Sci.* **2011**, *2*, 1178.
[69] D. Khodagholy, M. Gurfinkel, E. Stavrinidou, P. Leleux, T. Herve, S. Sanaur, G. G. Malliaras, *Appl. Phys. Lett.* **2011**, *99*, 163304.
[70] M. Sessolo, D. Khodagholy, J. Rivnay, F. Maddalena, M. Gleyzes, E. Steidl, B. Buisson, G. G. Malliaras, *Adv. Mater.* **2013**, *25*, 2135.
[71] D. Kuzum, H. Takano, E. Shim, J. C. Reed, H. Juul, A. G. Richardson, J. De Vries, H. Bink, M. A. Dichter, T. H. Lucas, D. A. Coulter, E. Cubukcu, B. Litt, *Nat. Commun.* **2014**, *5*, 5259.
[72] C. L. Weaver, J. M. Larosa, X. Luo, X. T. Cui, *ACS Nano* **2014**, *8*, 1834.
[73] K. A. Ng, E. Greenwald, Y. P. Xu, N. V. Thakor, *Med. Biol. Eng. Comput.* **2016**, *54*, 45.
[74] R. H. Olsson, D. L. Buhl, A. M. Sirota, G. Buzsaki, K. D. Wise, *IEEE Trans. Biomed. Eng.* **2005**, *52*, 1303.
[75] B. C. Raducanu, R. F. Yazicioglu, C. M. Lopez, M. Ballini, J. Putzeys, S. Wang, A. Andrei, M. Welkenhuysen, N. Van Helleputte, S. Musa, R. Puers, F. Kloosterman, C. Van Hoof, S. Mitra, in *2016 46th European Solid-State Device Research Conf.*, IEEE, Piscataway, NJ **2016**, pp. 385–388.
[76] R. R. Harrison, C. Charles, *IEEE J. Solid-State Circuits* **2003**, *38*, 958.
[77] R. Harrison, P. Watkins, R. Kier, R. Lovejoy, D. Black, R. Normann, F. Solzbacher, in *2006 IEEE Int. Solid State Circuits Conf.—Digest of Technical Papers*, IEEE, Piscataway, NJ **2006**, pp. 2258–2267.
[78] J. Cisneros-Fernández, M. Dei, L. Terés, F. Serra-Graells, in *2019 IEEE Int. Symp. on Circuits and Systems (ISCAS)*, IEEE, Piscataway, NJ **2019**, pp. 1–5.
[79] J. Viventi, D.-H. Kim, L. Vigeland, E. S. Frechette, J. A. Blanco, Y.-S. Kim, A. E. Avrin, V. R. Tiruvadi, S.-W. Hwang, A. C. Vanleer, D. F. Wulsin, K. Davis, C. E. Gelber, L. Palmer, J. Van der Spiegel, J. Wu, J. Xiao, Y. Huang, D. Contreras, J. A. Rogers, B. Litt, *Nat. Neurosci.* **2011**, *14*, 1599.
[80] A. Ballini, M. Muller, J. Livi, P. Chen, Y. Frey, U. Stettler, A. Shadmani, A. Viswam, V. Jones, I. J. Jackel, D. Radivojevic, M. Lewandowska, M. K. Gong, W. Fiscella, M. Bakkum, D. J. Heer, F. Hierlemann, *IEEE J. Solid-State Circuits* **2017**, *49*, 2705.
[81] M. G. Dorman, M. A. Prisbe, J. D. Meindl, *IEEE J. Solid-State Circuits* **1985**, *20*, 1185.
[82] K. Najafi, K. D. Wise, *IEEE J. Solid-State Circuits* **1986**, *21*, 1035.
[83] J. Müller, M. Ballini, P. Livi, Y. Chen, A. Shadmani, U. Frey, I. L. Jones, M. Fiscella, M. Radivojevic, D. J. Bakkum, in *2013 Transducers & Eurosensors XXVII: The 17th Int. Conf. on Solid-State Sensors, Actuators and Microsystems*, IEEE, Piscataway, NJ **2013**, pp. 744–747.
[84] H. Fang, K. J. Yu, C. Gloschat, Z. Yang, E. Song, C.-H. Chiang, J. Zhao, S. M. Won, S. Xu, M. Trumpis, Y. Zhong, S. W. Han, Y. Xue, D. Xu, S. W. Choi, G. Cauwenberghs, M. Kay, Y. Huang, J. Viventi, I. R. Efimov, J. A. Rogers, *Nat. Biomed. Eng.* **2017**, *1*, 38.
[85] H. Fang, J. Zhao, K. J. Yu, E. Song, A. B. Farimani, C.-H. Chiang, X. Jin, Y. Xue, D. Xu, W. Du, K. J. Seo, Y. Zhong, Z. Yang, S. M. Won, G. Fang, S. W. Choi, S. Chaudhuri, Y. Huang, M. A. Alam, J. Viventi, N. R. Aluru, J. A. Rogers, *Proc. Natl. Acad. Sci. USA* **2016**, *113*, 11682.
[86] A. Tsumura, H. Koezuka, T. Ando, *Appl. Phys. Lett.* **1986**, *49*, 1210.
[87] A. Tsumura, H. Koezuka, T. Ando, *Synth. Met.* **1988**, *25*, 11.
[88] H. Koezuka, A. Tsumura, *Synth. Met.* **1989**, *28*, 753.
[89] L. H. Hess, M. Jansen, V. Maybeck, M. V. Hauf, M. Seifert, M. Stutzmann, I. D. Sharp, A. Offenhäusser, J. A. Garrido, *Adv. Mater.* **2011**, *23*, 5045.
[90] C. Hébert, E. Masvidal-Codina, A. Suarez-Perez, A. B. Calia, G. Piret, R. Garcia-Cortadella, X. Illa, E. Del Corro Garcia, J. M. De la Cruz Sanchez, D. V. Casals, E. Prats-Alfonso, J. Bousquet, P. Godignon, B. Yvert, R. Villa, M. V. Sanchez-Vives, A. Guimerà-Brunet, J. A. Garrido, *Adv. Funct. Mater.* **2018**, *28*, 1703976.
[91] E. Masvidal-Codina, X. Illa, M. Dasilva, A. B. Calia, T. Dragojević, E. E. Vidal-Rosas, E. Prats-Alfonso, J. Martínez-Aguilar, J. M. De la Cruz, R. Garcia-Cortadella, P. Godignon, G. Rius, A. Camassa, E. Del Corro, J. Bousquet, C. Hébert, T. Durduran, R. Villa, M. V. Sanchez-Vives, J. A. Garrido, A. Guimerà-Brunet, *Nat. Mater.* **2019**, *18*, 280.
[92] D. Khodagholy, T. Doublet, P. Quilichini, M. Gurfinkel, P. Leleux, A. Ghestem, E. Ismailova, T. Hervé, S. Sanaur, C. Bernard, G. G. Malliaras, *Nat. Commun.* **2013**, *4*, 1575.
[93] D. A. D. A. Bernards, G. G. G. Malliaras, *Adv. Funct. Mater.* **2007**, *17*, 3538.
[94] G. D. Spyropoulos, J. N. Gelinas, D. Khodagholy, *Sci. Adv.* **2019**, *5*, eaau7378.
[95] C. Cea, G. D. Spyropoulos, P. Jastrzebska-Perfect, J. J. Ferrero, J. N. Gelinas, D. Khodagholy, *Nat. Mater.* **2020**, *19*, 679.
[96] T. Keller, A. Kuhn, *J. Autom. Control* **2008**, *18*, 35.
[97] G. D. Spyropoulos, J. Savarin, E. F. Gomez, D. T. Simon, M. Berggren, J. N. Gelinas, E. Stavrinidou, D. Khodagholy, *Adv. Mater. Technol.* **2019**, *5*, 1900652.
[98] R. A. Green, S. Baek, L. A. Poole-Warren, P. J. Martens, *Sci. Technol. Adv. Mater.* **2010**, *11*, 014107.
[99] Y. Liu, J. Liu, S. Chen, T. Lei, Y. Kim, S. Niu, H. Wang, X. Wang, A. M. Foudeh, J. B.-H. Tok, Z. Bao, *Nat. Biomed. Eng.* **2019**, *3*, 58.
[100] B. Lu, H. Yuk, S. Lin, N. Jian, K. Qu, J. Xu, X. Zhao, *Nat. Commun.* **2019**, *10*, 1043.
[101] J. Goding, C. Vallejo-Giraldo, O. Syed, R. Green, *J. Mater. Chem. B* **2019**, *7*, 1625.
[102] U. A. Aregueta-Robles, A. J. Woolley, L. A. Poole-Warren, N. H. Lovell, R. A. Green, *Front. Neuroeng.* **2014**, *7*, 15.
[103] C. J. Hartmann, S. Fliegen, S. J. Groiss, L. Wojtecki, A. Schnitzler, *Ther. Adv. Neurol. Disord.* **2019**, https://doi.org/10.1177/1756286419838096.
[104] A. Williamson, M. Ferro, P. Leleux, E. Ismailova, A. Kaszas, T. Doublet, P. Quilichini, J. Rivnay, B. Rózsa, G. Katona, C. Bernard, G. G. Malliaras, *Adv. Mater.* **2015**, *27*, 4405.
[105] X. Liu, M. Zhang, A. G. Richardson, T. H. Lucas, J. Van der Spiegel, *IEEE Trans. Biomed. Circuits Syst.* **2016**, *11*, 729.
[106] A. Zhou, S. R. Santacruz, B. C. Johnson, G. Alexandrov, A. Moin, F. L. Burghardt, J. M. Rabaey, J. M. Carmena, R. Muller, *Nat. Biomed. Eng.* **2019**, *3*, 15.

[107] J. Park, G. Kim, S. D. Jung, *IEEE Trans. Neural Syst. Rehabil. Eng.* **2017**, *25*, 2227.
[108] G. P. Seu, G. N. Angotzi, F. Boi, L. Raffo, P. Meloni, *IEEE Trans. Biomed. Circuits Syst.* **2018**, *12*, 839.
[109] U. Ziemann, *Neuroscience* **2011**, *17*, 368.
[110] M. Hallett, *Nature* **2000**, *406*, 147.
[111] Z. De Deng, S. H. Lisanby, A. V. Peterchev, *Brain Stimul.* **2013**, *6*, 1.
[112] M. C. Romero, M. Davare, M. Armendariz, P. Janssen, *Nat. Commun.* **2019**, *10*, 2642.
[113] G. Bonmassar, S. W. Lee, D. K. Freeman, M. Polasek, S. I. Fried, J. T. Gale, *Nat. Commun.* **2012**, *3*, 921.
[114] R. Chen, G. Romero, M. G. Christiansen, A. Mohr, P. Anikeeva, *Science* **2015**, *347*, 6.
[115] W. Legon, T. F. Sato, A. Opitz, J. Mueller, A. Barbour, A. Williams, W. J. Tyler, *Nat. Neurosci.* **2014**, *17*, 322.
[116] S. Ibsen, A. Tong, C. Schutt, S. Esener, S. H. Chalasani, *Nat. Commun.* **2015**, *6*, 8264.
[117] X. Wang, J. Song, J. Liu, Z. L. Wang, *Science* **2007**, *316*, 102.
[118] A. Marino, S. Arai, Y. Hou, E. Sinibaldi, M. Pellegrino, Y.-T. Chang, B. Mazzolai, V. Mattoli, M. Suzuki, G. Ciofani, *ACS Nano* **2015**, *9*, 7678.
[119] F. Marquet, Y. S. Tung, T. Teichert, V. P. Ferrera, E. E. Konofagou, *PLoS One* **2011**, *6*, 1.
[120] J. J. Choi, M. Pernot, S. A. Small, E. E. Konofagou, *Ultrasound Med. Biol.* **2007**, *33*, 95.
[121] K. Deisseroth, *Nat. Methods* **2010**, *8*, 1.
[122] L. He, Y. Zhang, G. Ma, P. Tan, Z. Li, S. Zang, X. Wu, J. Jing, S. Fang, L. Zhou, *eLife* **2015**, *4*, e10024.
[123] S. Il Park, D. S. Brenner, G. Shin, C. D. Morgan, B. A. Copits, H. U. Chung, M. Y. Pullen, K. N. Noh, S. Davidson, S. J. Oh, J. Yoon, K. I. Jang, V. K. Samineni, M. Norman, J. G. Grajales-Reyes, S. K. Vogt, S. S. Sundaram, K. M. Wilson, J. S. Ha, R. Xu, T. Pan, T. Il Kim, Y. Huang, M. C. Montana, J. P. Golden, M. R. Bruchas, R. W. Gereau, J. A. Rogers, *Nat. Biotechnol.* **2015**, *33*, 1280.
[124] M. Schwaerzle, K. Seidl, U. T. Schwarz, O. Paul, P. Ruther, in *2013 IEEE 26th Int. Conf. on Micro Electro Mechanical Systems (MEMS)*, IEEE, Piscataway, NJ **2013**, pp. 1029–1032.
[125] F. Wu, E. Stark, P.-C. Ku, K. D. Wise, G. Buzsáki, E. Yoon, *Neuron* **2015**, *88*, 1136.
[126] A. Mohanty, Q. Li, M. A. Tadayon, G. Bhatt, E. Shim, X. Ji, J. Cardenas, S. A. Miller, A. Kepecs, M. Lipson, arXiv1805.11663, **2018**.
[127] J. Lee, I. Ozden, Y. K. Song, A. V. Nurmikko, *Nat. Methods* **2015**, *12*, 1157.
[128] K. L. Montgomery, A. J. Yeh, J. S. Ho, V. Tsao, S. M. Iyer, L. Grosenick, E. A. Ferenczi, Y. Tanabe, K. Deisseroth, S. L. Delp, A. S. Y. Poon, *Nat. Methods* **2015**, *12*, 969.
[129] J. A. Rogers, T. Someya, Y. Huang, *Science* **2010**, *327*, 1603.
[130] H. Zhang, P. Gutruf, J. A. Rogers, in *Inorganic Flexible Optoelectronics: Materials and Applications* (Eds: Z. Ma, D. Liu), Wiley-VCH Verlag GmbH & Co. KGaA Weinheim, Germany, Weinheim **2019**, pp. 1–39.
[131] T. Sekitani, H. Nakajima, H. Maeda, T. Fukushima, T. Aida, K. Hata, T. Someya, *Nat. Mater.* **2009**, *8*, 494.
[132] C. Lu, U. P. Froriep, R. A. Koppes, A. Canales, V. Caggiano, J. Selvidge, E. Bizzi, P. Anikeeva, *Adv. Funct. Mater.* **2014**, *24*, 6594.
[133] S. Yoo, S. Hong, Y. Choi, J.-H. Park, Y. Nam, *ACS Nano* **2014**, *8*, 8040.
[134] J. L. Carvalho-de-Souza, J. S. Treger, B. Dang, S. B. H. Kent, D. R. Pepperberg, F. Bezanilla, *Neuron* **2015**, 1.
[135] K. Lugo, X. Miao, F. Rieke, L. Y. Lin, *Biomed. Opt. Express* **2012**, *3*, 447.
[136] D. Rand, M. Jakešová, G. Lubin, I. Vėbraitė, M. David-Pur, V. Đerek, T. Cramer, N. S. Sariciftci, Y. Hanein, E. D. Głowacki, *Adv. Mater.* **2018**, *30*, 1707292.
[137] M. Jakešová, M. Silverå Ejneby, V. Đerek, T. Schmidt, M. Gryszel, J. Brask, R. Schindl, D. T. Simon, M. Berggren, F. Elinder, E. D. Głowacki, *Sci. Adv.* **2019**, *5*, eaav5265.
[138] J. Isaksson, P. Kjäll, D. Nilsson, N. D. Robinson, M. Berggren, A. Richter-Dahlfors, *Nat. Mater.* **2007**, *6*, 673.
[139] A. Jonsson, S. Inal, L. Uguz, A. J. Williamson, L. Kergoat, J. Rivnay, D. Khodagholy, M. Berggren, C. Bernard, G. G. Malliaras, D. T. Simon, *Proc. Natl. Acad. Sci. USA* **2016**, *113*, E6903.
[140] R. van den Brand, J. Heutschi, Q. Barraud, J. DiGiovanna, K. Bartholdi, M. Huerlimann, L. Friedli, I. Vollenweider, E. M. Moraud, S. Duis, N. Dominici, S. Micera, P. Musienko, G. Courtine, *Science* **2012**, *336*, 1182.
[141] M. Asplund, C. Boehler, T. Stieglitz, *Front. Neuroeng.* **2014**, *7*, 9.
[142] I. R. Minev, P. Musienko, A. Hirsch, Q. Barraud, N. Wenger, E. M. Moraud, J. Gandar, M. Capogrosso, T. Milekovic, L. Asboth, R. F. Torres, N. Vachicouras, Q. Liu, N. Pavlova, S. Duis, A. Larmagnac, J. Vörös, S. Micera, Z. Suo, G. Courtine, S. P. Lacour, *Science* **2015**, *347*, 159.
[143] B. Rubehn, S. B. E. Wolff, P. Tovote, A. Lüthi, T. Stieglitz, *Lab Chip* **2013**, *13*, 579.
[144] J.-W. Jeong, J. G. McCall, G. Shin, Y. Zhang, R. Al-Hasani, M. Kim, S. Li, J. Y. Sim, K.-I. Jang, Y. Shi, D. Y. Hong, Y. Liu, G. P. Schmitz, L. Xia, Z. He, P. Gamble, W. Z. Ray, Y. Huang, M. R. Bruchas, J. A. Rogers, *Cell* **2015**, *162*, 662.
[145] A. Canales, X. Jia, U. P. Froriep, R. A. Koppes, C. M. Tringides, J. Selvidge, C. Lu, C. Hou, L. Wei, Y. Fink, P. Anikeeva, *Nat. Biotechnol.* **2015**, *33*, 277.
[146] T. Khaleeq, H. Hasegawa, M. Samuel, K. Ashkan, *Neuromodulation* **2019**, *22*, 489.
[147] J. D. Couch, A. M. Gilman, W. K. Doyle, *Neurosurgery* **2016**, *78*, 42.
[148] M. Azin, D. J. Guggenmos, S. Barbay, R. J. Nudo, P. Mohseni, *IEEE J. Solid-State Circuits* **2011**, *46*, 731.
[149] D. Seo, R. M. Neely, K. Shen, U. Singhal, E. Alon, J. M. Rabaey, J. M. Carmena, M. M. Maharbiz, *Neuron* **2016**, *91*, 529.
[150] S. Lee, H. Wang, Q. Shi, L. Dhakar, J. Wang, N. V. Thakor, S. C. Yen, C. Lee, *Nano Energy* **2017**, *33*, 1.
[151] U. M. Jow, M. Ghovanloo, *IEEE Trans. Biomed. Circuits Syst.* **2007**, *1*, 193.
[152] H. Zhang, P. Gutruf, K. Meacham, M. C. Montana, X. Zhao, A. M. Chiarelli, A. Vázquez-Guardado, A. Norris, L. Lu, Q. Guo, C. Xu, Y. Wu, H. Zhao, X. Ning, W. Bai, I. Kandela, C. R. Haney, D. Chanda, R. W. Gereau, J. A. Rogers, *Sci. Adv.* **2019**, *5*, eaaw0873.
[153] J. S. Ho, Y. Tanabe, S. M. Iyer, A. J. Christensen, L. Grosenick, K. Deisseroth, S. L. Delp, A. S. Y. Poon, *Phys. Rev. Appl.* **2015**, *4*, 024001.
[154] D.-H. Kim, N. Lu, R. Ma, Y.-S. Kim, R.-H. Kim, S. Wang, J. Wu, S. M. Won, H. Tao, A. Islam, K. J. Yu, T. Kim, R. Chowdhury, M. Ying, L. Xu, M. Li, H.-J. Chung, H. Keum, M. McCormick, P. Liu, Y.-W. Zhang, F. G. Omenetto, Y. Huang, T. Coleman, J. A. Rogers, *Science* **2011**, *333*, 838.
[155] M. Jakešová, T. A. Sjöström, V. Đerek, D. Poxson, M. Berggren, E. D. Głowacki, D. T. Simon, *npj Flexible Electron.* **2019**, *3*, 14.
[156] A. Wickens, B. Avants, N. Verma, E. Lewis, J. C. Chen, A. K. Feldman, S. Dutta, J. Chu, J. O'Malley, M. Beierlein, C. Kemere, J. T. Robinson, bioRxiv:*461855*, **2018**.
[157] K. Scholten, E. Meng, *Lab Chip* **2015**, *15*, 4256.
[158] A. A. Sharp, A. M. Ortega, D. Restrepo, D. Curran-Everett, K. Gall, *IEEE Trans. Biomed. Eng.* **2009**, *56*, 45.
[159] A. Prasad, Q. S. Xue, V. Sankar, T. Nishida, G. Shaw, W. J. Streit, J. C. Sanchez, *J. Neural Eng.* **2012**, *9*, 056015.
[160] K. M. Szostak, L. Grand, T. G. Constandinou, *Front. Neurosci.* **2017**, *11*, 665.
[161] A. Prasad, J. C. Sanchez, *J. Neural Eng.* **2012**, *9*, 026028.

[162] J. C. Barrese, N. Rao, K. Paroo, C. Triebwasser, C. Vargas-Irwin, L. Franquemont, J. P. Donoghue, *J. Neural Eng.* **2013**, *10*, 066014.
[163] D. Prodanov, J. Delbeke, *Front. Neurosci.* **2016**, *10*, 11.
[164] K. D. Wise, *IEEE Eng. Med. Biol. Mag.* **2005**, *24*, 22.
[165] G. Buzsáki, *Nat. Neurosci.* **2004**, *7*, 446.
[166] C. Pang, S. Musallam, Y.-C. Tai, J. W. Burdick, R. A. Andersen, in *2006 Int. Conf. on Microtechnologies in Medicine and Biology*, IEEE, Piscataway, NJ **2006**, pp. 64–67.
[167] A. Stett, B. Müller, P. Fromherz, *Phys. Rev. E - Stat. Physics, Plasmas, Fluids, Relat. Interdiscip. Top.* **1997**, *55*, 1779.
[168] S. T. Retterer, K. L. Smith, C. S. Bjornsson, K. B. Neeves, A. J. H. Spence, J. N. Turner, W. Shain, M. S. Isaacson, *IEEE Trans. Biomed. Eng.* **2004**, *51*, 2063.
[169] D. A. Henze, Z. Borhegyi, J. Csicsvari, A. Mamiya, K. D. Harris, G. Buzsáki, *J. Neurophysiol.* **2000**, *84*, 390.
[170] S. F. Cogan, D. J. Edell, A. A. Guzelian, Y. Ping Liu, R. Edell, *J. Biomed. Mater. Res.* **2003**, *67A*, 856.
[171] J. Park, V. Quaiserová-Mocko, K. Pecková, J. J. Galligan, G. D. Fink, G. M. Swain, *Diamond Relat. Mater.* **2006**, *15*, 761.
[172] H. Chan, D. M. Aslam, J. A. Wiler, B. Casey, *J. Microelectromech. Syst.* **2009**, *18*, 511.
[173] N. F. Nolta, M. B. Christensen, P. D. Crane, J. L. Skousen, P. A. Tresco, *Biomaterials* **2015**, *53*, 753.
[174] T. D. Y. Kozai, J. R. Eles, A. L. Vazquez, X. T. Cui, *J. Neurosci. Methods* **2016**, *258*, 46.
[175] S. Takeuchi, D. Ziegler, Y. Yoshida, K. Mabuchi, T. Suzuki, **2005**, *5*.
[176] S. P. Lacour, J. Jones, S. Wagner, T. Li, Z. Suo, *Proc. IEEE* **2005**, *93*, 1459.
[177] P. Hesketh, H.-S. Noh, K.-S. Moon, A. Cannon, P. J. Hesketh, C. P. Wong, *Artic. J. Micromech. Microeng.* **2004**.
[178] T. D. Yoshida Kozai, N. B. Langhals, P. R. Patel, X. Deng, H. Zhang, K. L. Smith, J. Lahann, N. A. Kotov, D. R. Kipke, *Nat. Mater.* **2012**, *11*, 1065.
[179] B. A. Wester, R. H. Lee, M. C. LaPlaca, *J. Neural Eng.* **2009**, *6*, 024002.
[180] H. P. Schwan, *Ann. N. Y. Acad. Sci.* **1968**, *148*, 191.
[181] S. Takeuchi, T. Suzuki, K. Mabuchi, H. Fujita, *J. Micromech. Microeng.* **2004**, *14*, 104.
[182] A. Mercanzini, K. Cheung, D. L. Buhl, M. Boers, A. Maillard, P. Colin, J.-C. Bensadoun, A. Bertsch, P. Renaud, *Sens. Actuators, A.* **2008**, *143*, 90.
[183] Y.-Y. Chen, H.-Y. Lai, S.-H. Lin, C.-W. Cho, W.-H. Chao, C.-H. Liao, S. Tsang, Y.-F. Chen, S.-Y. Lin, *J. Neurosci. Methods* **2009**, *182*, 6.
[184] E. Kim, J. Y. Kim, H. Choi, *Micro Nano Syst. Lett.* **2017**, *5*.
[185] B. Tian, J. Liu, T. Dvir, L. Jin, J. H. Tsui, Q. Qing, Z. Suo, R. Langer, D. S. Kohane, C. M. Lieber, *Nat. Mater.* **2012**, *11*, 986.
[186] A. Altuna, G. Gabriel, L. Menéndez de la Prida, M. Tijero, A. Guimerá, J. Berganzo, R. Salido, R. Villa, L. J. Fernández, *J. Micromech. Microeng.* **2010**, *20*, 064014.
[187] M. Tijero, G. Gabriel, J. Caro, A. Altuna, R. Hernández, R. Villa, J. Berganzo, F. J. Blanco, R. Salido, L. J. Fernández, *Biosens. Bioelectron.* **2009**, *24*, 2410.
[188] A. Colas, J. Curtis, in *Biomaterials Science* (Eds: B. D. Ratner, A. S. Hoffman, F. J. Schoen, J. E. Lemons), Elsevier, San Diego **2004**, pp. 80–86.
[189] F. Xu, Y. Zhu, *Adv. Mater.* **2012**, *24*, 5117.
[190] S. P. Lacour, D. Chan, S. Wagner, T. Li, Z. Suo, *Appl. Phys. Lett.* **2006**, *88*, 204103.
[191] C. Hassler, T. Boretius, T. Stieglitz, *J. Polym. Sci., Part B: Polym. Phys.* **2011**, *49*, 18.
[192] M. R. Abidian, D. C. Martin, *Adv. Funct. Mater.* **2009**, *19*, 573.
[193] A. E. Hess, J. R. Capadona, K. Shanmuganathan, L. Hsu, S. J. Rowan, C. Weder, D. J. Tyler, C. A. Zorman, *J. Micromech. Microeng.* **2011**, *21*, 054009.
[194] K. Shanmuganathan, J. R. Capadona, S. J. Rowan, C. Weder, *Prog. Polym. Sci.* **2010**, *35*, 212.
[195] N. A. Peppas, J. Z. Hilt, A. Khademhosseini, R. Langer, **2006**.
[196] T. Ware, D. Simon, D. E. Arreaga-Salas, J. Reeder, R. Rennaker, E. W. Keefer, W. Voit, *Adv. Funct. Mater.* **2012**, *22*, 3470.
[197] A. Zátonyi, G. Orbán, R. Modi, G. Márton, D. Meszéna, I. Ulbert, A. Pongrácz, M. Ecker, W. E. Voit, A. Joshi-Imre, Z. Fekete, *Sci. Rep.* **2019**, *9*, 2321.
[198] D.-H. Kim, J. Viventi, J. J. Amsden, J. Xiao, L. Vigeland, Y.-S. Kim, J. A. Blanco, B. Panilaitis, E. S. Frechette, D. Contreras, D. L. Kaplan, F. G. Omenetto, Y. Huang, K.-C. Hwang, M. R. Zakin, B. Litt, J. A. Rogers, *Nat. Mater.* **2010**, *9*, 511.
[199] O. J. Rauhala, S. Dominguez, G. D. Spyropoulos, J. J. Ferrero, T. R. Boyers, P. Jastrzebska-Perfect, C. Cea, D. Khodagholy, J. N. Gelinas, *Adv. Mater. Technol.* **2019**, *5*, 1900663.
[200] L. Yin, H. Cheng, S. Mao, R. Haasch, Y. Liu, X. Xie, S. W. Hwang, H. Jain, S. K. Kang, Y. Su, R. Li, Y. Huang, J. A. Rogers, *Adv. Funct. Mater.* **2014**, *24*, 645.
[201] E. Bat, Z. Zhang, J. Feijen, D. W. Grijpma, A. A. Poot, *Regener. Med.* **2014**, *9*, 385.
[202] J. Pas, A. L. Rutz, P. P. Quilichini, A. Slézia, A. Ghestem, A. Kaszas, M. J. Donahue, V. F. Curto, R. P. O'Connor, C. Bernard, A. Williamson, G. G. Malliaras, *J. Neural Eng.* **2018**, *15*, 065001.
[203] E. M. Schmidt, M. J. Bak, J. S. McIntosh, *Exp. Neurol.* **1976**, *52*, 496.
[204] R. J. Zdrahala, I. J. Zdrahala, *J. Biomater Appl.* **1999**, *14*, 67.
[205] L. Rao, H. Zhou, T. Li, C. Li, Y. Y. Duan, *Acta Biomater.* **2012**, *8*, 2233.
[206] N. Roohpour, A. Moshaverinia, J. M. Wasikiewicz, D. Paul, M. Wilks, M. Millar, P. Vadgama, *Biomed. Mater.* **2012**, *7*, 015007.
[207] R. DeIasi, J. Russell, *J. Appl. Polym. Sci.* **1971**, *15*, 2965.
[208] P. Takmakov, K. Ruda, K. Scott Phillips, I. S. Isayeva, V. Krauthamer, C. G. Welle, *J. Neural Eng.* **2015**, *12*, 026003.
[209] G. T. Hwang, D. Im, S. E. Lee, J. Lee, M. Koo, S. Y. Park, S. Kim, K. Yang, S. J. Kim, K. Lee, K. J. Lee, *ACS Nano* **2013**, *7*, 4545.
[210] J. Jeong, S. Hyun Bae, J. M. Seo, H. Chung, S. June Kim, *J. Neural Eng.* **2016**, *13*, 025004.
[211] J. Jeong, K. S. Min, S. J. Kim, *Microelectron. Eng.* **2019**, *216*, 111096.
[212] S. W. Lee, F. Fallegger, B. D. F. Casse, S. I. Fried, *Sci. Adv.* **2016**, *2*, e1600889.
[213] C. Jae Lee, S. Jae Oh, J. Keun Song, S. June Kim, *Mater. Sci. Eng. C* **2004**, *24*, 265.
[214] J.-M. Hsu, L. Rieth, R. A. Normann, P. Tathireddy,F. Solzbacher, *IEEE Trans. Biomed. Eng.* **2009**, *56*, 23.
[215] W. M. Tsang, A. L. Stone, Z. N. Aldworth, J. G. Hildebrand, T. L. Daniel, A. I. Akinwande, J. Voldman, *IEEE Trans. Biomed. Eng.* **2010**, *57*, 1757.
[216] P. J. Rousche, D. S. Pellinen, D. P. Pivin, J. C. Williams, R. J. Vetter, D. R. Kipke, *IEEE Trans. Biomed. Eng.* **2001**, *48*, 361.
[217] F. Pothof, L. Bonini, M. Lanzilotto, A. Livi, L. Fogassi, G. A. Orban, O. Paul, P. Ruther, *J. Neural Eng.* **2016**, *13*, 046006.
[218] W. Li, D. C. Rodger, A. Pinto, E. Meng, J. D. Weiland, M. S. Humayun, Y.-C. Tai, *Sens. Actuators, A.* **2011**, *166*, 193.
[219] G. Hong, X. Yang, T. Zhou, C. M. Lieber, *Curr. Opin. Neurobiol.* **2018**, *50*, 33.
[220] D.-W. W. Park, A. A. Schendel, S. Mikael, S. K. Brodnick, T. J. Richner, J. P. Ness, M. R. Hayat, F. Atry, S. T. Frye, R. Pashaie, S. Thongpang, Z. Ma, J. C. Williams, *Nat. Commun.* **2014**, *5*, 5258.
[221] M. Park, J. Park, U. Jeong, *Nano Today* **2014**, *9*, 244.
[222] J. Zhang, X. Liu, W. Xu, W. Luo, M. Li, F. Chu, L. Xu, A. Cao, J. Guan, S. Tang, X. Duan, *Nano Lett.* **2018**, *18*, 2903.
[223] N. Matsuhisa, M. Kaltenbrunner, T. Yokota, H. Jinno, K. Kuribara, T. Sekitani, T. Someya, *Nat. Commun.* **2015**, *6*, 7461.

[224] J. Tang, H. Guo, M. Zhao, J. Yang, D. Tsoukalas, B. Zhang, J. Liu, C. Xue, W. Zhang, *Sci. Rep.* **2015**, *5*, 16527.
[225] J. A. Fan, W.-H. Yeo, Y. Su, Y. Hattori, W. Lee, S.-Y. Jung, Y. Zhang, Z. Liu, H. Cheng, L. Falgout, M. Bajema, T. Coleman, D. Gregoire, R. J. Larsen, Y. Huang, J. A. Rogers, *Nat. Commun.* **2014**, *5*, 3266.
[226] W. Wu, *Sci. Technol. Adv. Mater.* **2019**, *20*, 187.
[227] P. Norlin, M. Kindlundh, A. Mouroux, K. Yoshida, U. G. Hofmann, *J. Micromech. Microeng.* **2002**, *12*, 414.
[228] H. G. Kim, K. Kim, E. Lee, T. An, W. Choi, G. Lim, H. J. Shin, *Mater.* **2018**, *11*.
[229] C. K. Bjune, T. F. Marinis, J. M. Brady, J. Moran, J. Wheeler, T. S. Sriram, P. D. Parks, A. S. Widge, D. D. Dougherty, E. N. Eskandar, in *Proc. of the Annual Int. Conf. of the IEEE Engineering in Medicine and Biology Society*, IEEE, Piscataway, NJ **2015**, pp. 7825–7830.
[230] D.-H. Baek, J. S. Park, E.-J. Lee, S. J. Shin, J.-H. Moon, J. J. Pak, S.-H. Lee, *IEEE Trans. Biomed. Eng.* **2011**, *58*, 1466.
[231] P. Jastrzebska-Perfect, G. D. Spyropoulos, C. Cea, Z. Zhao, J. Onni, A. Viswanathan, S. A. Sheth, J. N. Gelinas, D. Khodagholy, *Sci. Adv.* **2020**, *6*, eaaz6767.
[232] R. Fiáth, B. C. Raducanu, S. Musa, A. Andrei, C. M. Lopez, C. van Hoof, P. Ruther, A. Aarts, D. Horváth, I. Ulbert, *Biosens. Bioelectron.* **2018**, *106*, 86.
[233] A. A. Fomani, R. R. Mansour, *Sens. Actuators, A.* **2011**, *168*, 233.
[234] M. R. Abidian, J. M. Corey, D. R. Kipke, D. C. Martin, *Small* **2010**, *6*, 421.
[235] D. Khodagholy, T. Doublet, M. Gurfinkel, P. Quilichini, E. Ismailova, P. Leleux, T. Herve, S. Sanaur, C. Bernard, G. G. Malliaras, *Adv. Mater.* **2011**, *23*, H268.
[236] E. Ben-Jacob, Y. Hanein, *J. Mater. Chem.* **2008**, *18*, 5181.
[237] W. Lee, D. Kim, N. Matsuhisa, M. Nagase, M. Sekino, G. G. Malliaras, T. Yokota, T. Someya, *Proc. Natl. Acad. Sci. USA* **2017**, *114*, 10554.
[238] J. Buhlmann, L. Hofmann, P. Tass, C. Hauptmann, *Front. Neuroeng.* **2011**, *4*, 15.
[239] Y. Son, H. J. Lee, J. Kim, H. Shin, N. Choi, C. Justin Lee, E. S. Yoon, E. Yoon, K. D. Wise, T. G. Kim, I. J. Cho, *Sci. Rep.* **2015**, *5*, 15466.
[240] P. Anikeeva, Optoelectronic fibers interrogate brain function. *SPIE News* **2015**.
[241] S. Park, S. W. Heo, W. Lee, D. Inoue, Z. Jiang, K. Yu, H. Jinno, D. Hashizume, M. Sekino, T. Yokota, K. Fukuda, K. Tajima, T. Someya, *Nature* **2018**, *561*, 516.
[242] Z. Zhao, L. Luan, X. Wei, H. Zhu, X. Li, S. Lin, J. J. Siegel, R. A. Chitwood, C. Xie, *Nano Lett.* **2017**, *17*, 4588.
[243] D. Lee, H. C. Moon, B.-T. Tran, D.-H. Kwon, Y. H. Kim, S.-D. Jung, J. H. Joo, Y. S. Park, *Exp. Neurobiol.* **2018**, *27*, 593.
[244] M. B. Christensen, S. M. Pearce, N. M. Ledbetter, D. J. Warren, G. A. Clark, P. A. Tresco, *Acta Biomater.* **2014**, *10*, 4650.
[245] T. Kawano, T. Harimoto, A. Ishihara, K. Takei, T. Kawashima, S. Usui, M. Ishida, *Biosens. Bioelectron.* **2010**, *25*, 1809.
[246] T. D. Y. Kozai, Z. Gugel, X. Li, P. J. Gilgunn, R. Khilwani, O. B. Ozdoganlar, G. K. Fedder, D. J. Weber, X. T. Cui, *Biomaterials* **2014**, *35*, 9255.
[247] T. D. Y. Kozai, D. R. Kipke, *J. Neurosci. Methods* **2009**, *184*, 199.
[248] J. Reeder, M. Kaltenbrunner, T. Ware, D. Arreaga-Salas, A. Avendano-Bolivar, T. Yokota, Y. Inoue, M. Sekino, W. Voit, T. Sekitani, T. Someya, *Adv. Mater.* **2014**, *26*, 4967.
[249] M. Leber, J. Körner, C. F. Reiche, M. Yin, R. Bhandari, R. Franklin, S. Negi, F. Solzbacher, in *Neural Interface: Frontiers and Applications* (Ed: X. Zheng), Springer, Singapore **2019**, pp. 1–40.
[250] C.-H. Chen, C.-T. Lin, W.-L. Hsu, Y.-C. Chang, S.-R. Yeh, L.-J. Li, D.-J. Yao, *Nanomed.: Nanotechnol., Biol. Med.* **2013**, *9*, 600.
[251] D. Khodagholy, J. N. Gelinas, G. Buzsáki, *Science* **2017**, *358*, 369.
[252] D.-Y. Khang, H. Jiang, Y. Huang, J. A. Rogers, *Science* **2006**, *311*, 208.
[253] S. Ayub, L. J. Gentet, R. Fiáth, M. Schwaerzle, M. Borel, F. David, P. Barthó, I. Ulbert, O. Paul, P. Ruther, *Biomed. Microdevices* **2017**, *19*, 49.
[254] J. Du, T. J. Blanche, R. R. Harrison, H. A. Lester, S. C. Masmanidis, *PLoS One* **2011**, *6*, e26204.
[255] R. C. Kelly, M. A. Smith, J. M. Samonds, A. Kohn, A. B. Bonds, J. A. Movshon, S. L. Tai, *J. Neurosci.* **2007**, *27*, 261.
[256] S. Belverud, A. Mogilner, M. Schulder, *Neurotherapeutics* **2008**, *5*, 114.
[257] T. D. Y. Kozai, *Micromachines* **2018**, *9*, 1.
[258] B. Lee, M. N. Zubair, Y. D. Marquez, D. M. Lee, L. A. Kalayjian, C. N. Heck, C. Y. Liu, *World Neurosurg.* **2015**, *84*, 719.
[259] S. Musallam, M. J. Bak, P. R. Troyk, R. A. Andersen, *J. Neurosci. Methods* **2007**, *160*, 122.
[260] Intan Technologies, http://intantech.com/products_RHD2000.html (accessed: April 2020).